VIRUS - INDUCED ER STRESS IN PLANTS

By

OMAR PAUL ARIAS GAGUANCELA

Bachelor of Science in Biotechnology

University of the Armed Forces - ESPE

Quito, Ecuador

2014

Submitted to the Faculty of the
Graduate College of the
Oklahoma State University
in partial fulfillment of
the requirements for
the Degree of
MASTER OF SCIENCE
July, 2017

VIRUS - INDUCED ER STRESS IN PLANTS

Thesis Approved:

Dr. Jeanmarie Verchot

Thesis Adviser

Dr. Nathan Walker

Committee Member

Dr. Carla Garzon

Committee Member

ACKNOWLEDGEMENTS

Name: OMAR PAUL ARIAS GAGUANCELA

Date of Degree: JULY, 2017

Title of Study: VIRUS - INDUCED ER STRESS IN PLANTS

Major Field: ENTOMOLOGY AND PLANT PATHOLOGY

Abstract: The endoplasmic reticulum (ER) is a membrane system that acts as platform for RNA viral replication and movement. The potexvirus TGB3 and potyvirus 6K2 proteins cause alterations in the ER architecture and protein production, causing ER stress. Embedded in the ER membrane are ER stress sensors that detect malformed proteins and elicit signaling cascades that result in changes in nuclear gene expression, process known as unfolded protein response (UPR). The most conserved ER stress sensors are IRE1 (coded by *IRE1a* and *IRE1b*), and type II transmembrane (bZIP) named bZIP60, bZIP17 and bZIP28 transcription factors which enter the nucleus to recognize promoters to activate gene expression of chaperone binding protein (BiP) to restore homeostasis. BI-1 is a cell death suppressor that resides in the ER and is believed to be downstream of IRE1. The contribution of these ER sensors in virus pathogenicity is poorly understood. This study revealed that knockdown of ER stress sensors leads to greater plant virus accumulation. PlAMV-GFP and TuMV-GFP accumulated to higher levels in *Arabidopsis* plants defective for both *IRE1a* and *IRE1b* than in wild-type Col-O. Interestingly, *bZIP60* was a host susceptibility factor for both viruses, whereas *bZIP28* and *bZIP17* knockouts differentially accumulated PlAMV-GFP and TuMV-GFP in *Arabidopsis* plants. Agro-delivery of potexvirus TGB3 and potyvirus 6K2 resulted in elevated *bZIP60, bZIP28* and *bZIP17* transcript levels in *Arabidopsis* and *N. benthamiana* plants, which led to *BiP* gene activation. *Arabidopsis* plants defective for *BI-1* were found to have a more significant effect on systemic PlAMV-GFP and TuMV-GFP accumulation than in *bZIP60* mutant plants. Similarly, the experiments conducted in *BI-1* and *bZIP60* silenced *N. benthamiana* plants infected with PVX-GFP or PVY-GFP showed that knockdown of *BI-1* produced higher virus accumulation levels than *bZIP60*. This data suggest that UPR pathways provide some protection against virus infection.

TABLE OF CONTENTS

LIST OF TABLES

LIST OF FIGURES

Figure   Page

CHAPTER I

INTRODUCTION AND OBJECTIVES

Introduction

The endoplasmic reticulum (ER) is a membrane system that acts as platform for RNA viral replication and movement. Potexviruses are RNA viruses, members of the family Alphaflexiviridae which have a module of three overlapping open reading frames (ORFs) called the "triple gene block" (TGB). These three movement proteins are known as TGB1, TGB2 and TGB3 and enable movement of viral RNA between neighboring cells through plasmodesmata (Bamunusinghe *et al.*, 2009). During potexvirus infection with *Potato virus X* (PVX), the TGB2 and TGB3 proteins reside in the ER and cause alterations in the ER architecture including the formation of vesicles (Ju *et al.*, 2007). Prior research also indicated that TGB3 specifically activates a signal cascade that alters host gene expression. This cascade is led by ER resident stress sensors. Potyviruses are RNA viruses and members of the Potyviridae and their genomes encode one long open reading frame that generates a polyprotein. The polyprotein is cleaved to produce 11 mature products, one of which is known as the 6K2 protein. The 6K2 protein resides in the ER and causes alterations in the membrane structure that includes formation of vesicles (Jiang *et al.*, 2015).

The 6K2 protein from TuMV anchors the viral replicase to the ER and induces the formation of vesicles that are crucial for the movement of viral RNA and replication proteins (Spetz *et al.*, 2004; Cotton *et al.*, 2009). The potexvirus TGB3 and the potyvirus 6K2 have a single transmembrane domain at the N-terminus (Grangeon *et al.*, 2013; Jiang *et al.*, 2015). It has been reported that the *Potato virus X* TGB3 and the *Turnip mosaic virus* 6K2 proteins activate the IRE1/bZIP60 signaling cascade in a manner that regulates virus infection (Ye *et al.*, 2011; Ye *et al.*, 2013; Zhang *et al.*, 2015; Arias Gaguancela *et al.*, 2016).

The ER plays a central role in protein synthesis, as well as carbohydrates and lipids assembling (Duwi Fanata *et al.*, 2013). To enable protein folding and maturation, the ER contains several resident molecular chaperones including ER luminal binding protein (BiP), calnexin (CNX), calmodulin (CAM) and calreticulin (CRT) (Williams *et al.*, 2014a). External factors like drought stress, salt stress, or virus infection can lead to increased translation of proteins and accumulation of malformed proteins in the ER, causing ER stress (Duwi Fanata *et al.*, 2013). Malformed proteins elicit a response by protein chaperones in the ER to refold these proteins or dispose of them. Embedded in the ER membrane are ER stress sensors that detect malformed proteins in the ER and elicit signaling cascades that result in changes in nuclear gene expression, process known as unfolded protein response (UPR). These genetic responses are specifically activated to increase the ER capacity to fold and dispose of proteins (Hollien, 2013). The most conserved ER stress sensor that provide adaptive responses to malformed proteins in the ER include the endoribonuclease inositol-requiring enzyme 1 (IRE1) (Chen *et al.*, 2013). *Arabidopsis thaliana* has encodes *IRE1a* and *IRE1b* which interact with malformed proteins in the ER, and are activated to mediate the splicing of a short intron and frameshift of mRNA basic leucine-zipper (bZIP) 60 transcription factor (Ruberti *et al.*, 2015). The truncated bZIP60 protein enters the nucleus and upregulates expression of genes that contain plant unfolded protein response elements (P-UPRE) in the promoter (Deng *et al.*, 2013a; Korner *et al.*, 2015).

Two additional transcription factors are tethered to the ER, and upon stress are re-directed to the nucleus to activate gene expression. These include the type II transmembrane (bZIP) named bZIP17 and bZIP28 (Schäfer *et al.*, 2012; Williams *et al.*, 2014a). The bZIP17 and bZIP28 proteins are tethered to the ER by BiP. During the UPR, BiP moves to the site of the malformed protein and refolds it, releasing bZIP17 and bZIP28. These transcription factors then are translocated to the Golgi apparatus where their transmembrane anchors are removed by the site 1 protease (S1P). The truncated bZIP17 and bZIP28 proteins move to the nucleus where they activate gene expression. Once in the nucleus these bZIP transcription factors will recognize promoters that contain the ER stress responsive *cis* element (ERSE-1) and P-UPRE (Duwi Fanata *et al.*, 2013).

Bax inhibitor 1 (BI-1), the Bcl2-associated athanogene (BAG) proteins BAG6 and BAG7, and S-phase kinase associated protein 1 (SKP1) are factors associated with protein turnover and cell death regulation (Reape *et al.*, 2008). BI-1 is an ER-resident membrane protein that is highly conserved in eukaryotes and plays a role in plant defense. The *atbi-1* mutant *A. thaliana* plants have showed increase susceptibility to *Fusarium graminearum* (Ishikawa *et al.*, 2011a).

The goal of this research was to investigate the interactions of the TGB3 and 6K2 proteins with the IRE1/bZIP60 and bZIP17, bZIP28 pathways. The second goal was to broadly examine viral interactions with factors involved in cell death and immune regulation that are also linked in some way to ER stress and protein turnover BI-1.

Objectives

1) Evaluate the contribution of UPR regulators *IRE1a*, *IRE1b, bZIP60, bZIP28* and *bZIP17* during infection of potexviruses and potyviruses in *A. thaliana* to determine if potyviruses and potexviruses interact with these machinery in similar or unique ways.

2) Analyze BiP genes induction to TGB3 and 6K2 viral proteins in *A. thaliana*, *N. benthamiana* and *S. tuberosum* in order to understand their role during UPR regulation.

3) Determine if systemic virus accumulation and necrosis are impacted by knocking down host gene expression of *bZIP60* and *BI-1* in *N. benthamiana*.

4) Investigate the interactions involving potyvirus 6K2 or potexvirus TGB3 viral proteins that enable *IRE1/bZIP60* and *BI-1* recognition of these elicitors to determine if similar factors are activated by these viruses.

CHAPTER II

REVIEW OF LITERATURE

Potexvirus genome

The potexvirus genome is characterized by the presence of five open reading frames (ORFs) flanked by a 5' methyl guanosine cap and a 3' poly (A) tail. The first ORF encodes the replicase (RNA-dependent RNA polymerase) protein that contains three activity domains: methyltransferase, helicase and RNA dependent RNA polymerase (Komatsu *et al.*, 2008; Komatsu *et al.*, 2011). This viral replicase is translated from the (+) ssRNA. The second, third and fourth ORFs encode the "triple gene block" (TGB1, TGB2, and TGB3) movement proteins (Huang *et al.*, 2004). The TGB1 protein is translated from subgenomic RNA (sgRNA) 1 while sgRNA2 is responsible for translation of TGB2 and TGB3. TGB1 has a helicase domain and its functions include suppression of RNA silencing, expansion of plasmodesmata, and membranes remodeling. TGB2 and TGB3 have ER binding domains and they are responsible for cell to cell movement (Tilsner *et al.*, 2012; Heinlein, 2015). The fifth ORF encodes the coat protein (CP) which is located close to the 3' end of the genome is translated from sgRNA3. CP is involved in encapsidation and movement (Tilsner *et al.*, 2013; Park *et al.*, 2014).

Life cycle of potexvirus

Infection begins when virion particles disassemble in the cellular cytoplasm and release the genomic (+) ssRNA. From this step, (+) RNA recruits host ribosomes and translation of genomic RNA produces the viral replicase. Viral replication complexes (VRCs) form along the ER (Park *et al.*, 2014). The VRCs lead the synthesis of (–) ssRNA which later is used as a template for the production of (+) ssRNA and three subgenomic (+) ssRNA. The first two subgenomic (+) ssRNAs will execute translation of the "triple gene block" proteins while the third subgenomic (+) ssRNA will encode the coat protein (Johnson *et al.*, 2003; Tilsner *et al.*, 2013). The RNA helicase activity of TGB1 will support unwinding between template (–) ssRNA and newly synthesized (+) ssRNA. TGB1 also will associate to CP and (+) ssRNA to form the ribonucleoprotein (RNP) complex or virus like particles which might be transported to neighboring cells (Solovyev *et al.*, 2012; Park *et al.*, 2013; Park *et al.*, 2014).

Cell to cell movement of potexvirus

One of the most accepted models for virus trafficking into other cells states that TGB2 derived vesicles recruit TGB3 and both direct the movement of vesicles from the perinuclear to the cortical side of the ER. TGB2 and TGB3 vesicles align on actin filaments to organize and lead to movement of ribonucleoprotein (RPN) complexes throughout the plasmodesmata (Schoelz *et al.*, 2011; Park *et al.*, 2013; Tilsner *et al.*, 2013). TGB1 which is a member of the RPN, might also be collaborating in expansion of the plasmodesmata pore size which will ultimately support cell to cell movement (Chou *et al.*, 2013).

Potyvirus genome

The potyvirus genome organization encodes a single genome length ORF flanked by a 5' VPg and a 3' poly (A) tail and a small ORF. The large ORF translates a polyprotein composed by

the viral proteins P1, HC-Pro, P3, 6K1, CI, 6K2, Nla-VPg, NIa-Pro, NIb and CP. The small ORF codes for the viral protein P3N-PIPO (Ivanov *et al.*, 2014; Cui *et al.*, 2016). P1 is a protease that cleaves itself from the polyprotein by its C-terminal. P1 functions include enhancement of silencing activity of HC-Pro and systemic spread (Nummert *et al.*, 2017). HC-Pro is a protease that cleaves itself from the polyprotein and functions as a suppressor of host RNA silencing (Mlotshwa *et al.*, 2016; Yang *et al.*, 2016). P3 is involved in RNA replication and has a small ORF embedded in it that encodes PIPO. By ribosomal frameshifting, which is a genome strategy to produce two proteins with overlapping ORFs, P3N-PIPO is produced. P3N-PIPO activity has been correlated with replication and virus movement into systemic tissues (Chung *et al.*, 2008). The exact function of 6K1 is not well described in the literature, although recent reports suggest its role in virus replication (Cui *et al.*, 2016). CI has ATPase and RNA helicase activities. CI participates in virus replication activity and virus adaptation in the host (Sorel *et al.*, 2014b). 6K2 anchors and associates with the ER to induce the formation of vesicles that will serve as replication complexes, furthermore 6K2 activity might include cell to cell movement (Jiang *et al.*, 2015). The genome-linked viral protein (VPg-Pro) has ATPase activity at the N-terminal domain and a C-terminal protease domain. NIa-Pro is essential for maturation cleavage of sites located on each side of 6K1, Cl, 6K2, VPg, NIa-Pro, NIb and CP. NIb is the replicase (RNA-dependent RNA polymerase). CP functions for encapsidation and protection of the new progeny of virions (Ivanov *et al.*, 2012; Ivanov *et al.*, 2014).

Life cycle of potyvirus

Potyvirus entry into cells is followed by uncoating, translation of (+) ssRNA to produce the polyprotein, formation of virus replication complexes (VRCs) and delivery of the viral progeny. The formation of the VRCs start with the 6K2 protein interaction with the NIa-Pro, tethering it to the ER. In turn, NIa –Pro recruits NIb to initiate the synthesis of (-) ssRNA. The 6K2 hijacks the membranes from the ER and the Golgi apparatus forming unique vesicles that

house and protect the VRCs (Jiang *et al.*, 2015). P3 also seems to be involved in the formation of VRCs, since both P3 and 6K2 have been shown to be co-localized in the ER (Cui *et al.*, 2010). The (-) ssRNA that is produced in the VRC, serves as a template for the synthesis of (+) ssRNA. The double strand RNA complexes are unwound by the RNA helicase activity of CI (Sorel *et al.*, 2014a; Sorel *et al.*, 2014b). Then, the newly synthesized (+) ssRNA starts new cycles of translation, replication or can be directed to plasmodesmata to infect other cells (Hong *et al.*, 2007; Ivanov *et al.*, 2014).

Cell to cell movement of potyvirus

The current model suggests that the (+) ssRNA synthesized in the VRC complexes associates to the CP to form ribonucleoprotein (RPN) complexes which will be mobilized to the plasmodesmata along actin filaments. The CP seems to recognize the viral protein CI which allows targeting to the plasmodesmata (Heinlein, 2015). P3N-PIPO also localizes along the plasmodesmata, modulates the formation of cylindrical inclusions at the periphery and facilities movement of the virus. This information supports the notion that potyvirus mobilization is carried out in RNP complexes facilitated by CI and P3N-PIPO rather than in fully encapsidated virions (Wei *et al.*, 2010).

Virus movement into systemic plant tissues

Virus infection into heathy leaves is a process that is mediated by mechanical inoculation or insect vector transmission. Virus spread include short and long distance movements (Hipper *et al.*, 2013). Short distance movement includes cell to cell transportation along nonvascular tissues (epidermis and mesophyll), process that is mediated by plasmodesmata and viral movement proteins such as potyvirus 6K2 and potexvirus "triple gene block" proteins (Verchot-Lubicz *et al.*, 2007; Schoelz *et al.*, 2011; Ivanov *et al.*, 2014). For viruses to reach systemic tissues (long distance movement), they need to reach vascular tissues to multiply in new infection sites. For

such purposes, plant viruses have to move through bundle sheath cells, vascular parenchyma and companion cells, in order to reach sieve elements in the phloem. Transportation through sieve elements is mediated by pore plasmodesmal units which reportedly have wider size pores than regular plasmodesmata. Vascular movement of the virus follows a source (infection foci) to sink (healthy leaves) flux, but it is important to mention that the direction and speed of the viral systemic movement will depend on several factors, such as virus host protein interactions, host resistance and the number of initial infection foci produced (Cheng *et al.*, 2000; Silva *et al.*, 2002; Hipper *et al.*, 2013; Rodrigo *et al.*, 2014).

The study of virus movement has been successful thanks to the used of gene reporter GFP (green fluorescent protein). The use of plant reference models infected with GFP tagged viral infectious clones are highly helpful to monitor virus long distance and short movement in plant tissues, thus proportioning an understanding of virus spread mechanisms and plant-host interactions (Serrano *et al.*, 2008; Harries *et al.*, 2011).

ER stress during viral infection

Potexvirus TGB3 and potyvirus 6K2 are involved in the activation of ER transcription factor bZPI60 thus enabling UPR responses via IRE1-bZIP60 cascade. Moreover it has also been seen that the presence of these two viral proteins are linked with the induction of binding protein (BiP) (Williams *et al.*, 2014b; Verchot, 2016). Given the interaction of TGB3 and 6K2 with UPR, it is not clear if these genes enhance or inhibit virus infection. Recent literature, has shown that chaperone CDC48 is induced upon tobacco mosaic virus treatment in *A. thaliana*, the same chaperone was capable of targeting and moving viral movement proteins out of the ER for degradation purposes, thereby reducing viral infection rate (Niehl *et al.*, 2012). This example highlighted the role of UPR genes in diminishing virus pathogenicity. In contrast in other studies, activation of IRE1 cascade in the ER is linked with virus replication promoting. For example, a

yeast UPR chaperone homolog of HSP70 has been shown to be activated upon viral infection, the upregulation of this chaperone in this case apparently enhances virus replication (Aparicio *et al.*, 2005; Zhang *et al.*, 2015). As observed in the examples given above, there is contradictory information about virus host interactions in the ER. This will hamper the knowledge about this particular topic and will affect further possibilities of designing and developing more virus disease tolerant crops which will ultimately lead to an eventual benefit in crop yields affected by plant viruses.

CHAPTER III

MATERIALS AND METHODS

Plasmids and bacterial strains

All plasmids were maintained in *Agrobacterium tumefaciens* strain GV3101. Infectious clones of several potyviruses and potexviruses tagged with the green fluorescent protein (GFP), were used to visualize viral movement in plants. pCAMBIA binary plasmids containing *Cauliflower mosaic virus* (CaMV) 35S promoter and GFP tagging infectious clones of *Turnip mosaic virus* (TuMV) provided by Dr. Aiming Wang (Southern Crop Protection and Food Research Center – Ontario, Canada) and *Plantago asiatica mosaic virus* (PlAMV) derived from non-necrotic strain Lily – isolate Li6 (Komatsu *et al.*, 2008) were used for infecting *Arabidopsis thaliana*. Additionally, a PVX-GFP infectious clone was obtained from Dr. Peter Moffett. The cDNAs of *Potato virus Y* (PVY) N605 strain genome were contained in pGR106/7 binary plasmids. GFP was inserted into these genomes (Hu *et al.*, 2011; Vassilakos *et al.*, 2016). The pMDC32 binary plasmids expressing the PVY 6K2, TuMV 6K2, PVX TGB3 and PlAMV TGB3 genes were also obtained (Curtis *et al.*, 2003; Arias Gaguancela *et al.*, 2016).

In addition pHellsgate-*bi1si* and pHellsgate-*bzip60si* constructs were prepared by Dr. Dennis Halterman at the USDA and used for silencing experiments in *Nicotiana benthamiana*. Both *BI-1* and *bZIP60* gene sequences used for the assembly of the silencing constructs were derived from PVY-resistant *S. chacoense* clone 39-7 (Arias Gaguancela *et al.*, 2016).

Plant material and agroinfiltration

Arabidopsis thaliana ecotype Col-O and homozygous (T-DNA) plant lines *ire1a-2* (SALK_018112), *ire1b-4* (SAIL_238_F07), *ire1a-2/1b-4, bzip60-1* (SALK_050203; locus At1g42990), and *bi1-2* (CS323793; locus At5G47120), *bzip17* (SALK_104326), *bzip28-2* (SALK_132285), *bzip17/bzip60* and *bzip28/bzip60* were obtained from the *Arabidopsis* Information Resource Center (Ohio State University, 055 Rightmire Hall and Carmack Rd, Columbus, OH).

N. benthamiana plants were used as a hosts for study of virus infection and for carrying out transient assays for silencing of *BI-1* and *bZIP60* genes. *Solanum tuberosum* cultivar Katahdin plants were propagated in Murashige and Skoog (MS) medium and were used to inoculate with PVX-GFP or PVY-GFP. All plant species were grown in growth chambers with 10 h light and 14 h of dark at 23 °C and after three weeks were subjected to *A. tumefaciens* infiltration which was conducted as follows: *A. tumefaciens* harboring the viral constructs grew on YEP media plates and then selected in liquid YEP media at 28 °C, 235 rpm for 16 hours. Cultures were pelleted by centrifugation for 5 min at 5000 rpm. Then, the supernatant was discarded and the pellet re-suspended in infiltration media (10 mM Mg_2SO_4, 10 mM MES) brought to pH=5.6 with acetosyringone (5 mM). The absorbance was adjusted to OD600= 0.5 to 1.0; finally the *A. tumefaciens* solution was incubated at room temperature for one hour and then infiltrated on the abaxial side of the leaf using a needle-free syringe.

Immunoblot analysis

Immunoblot analysis for detection of potexvirus and potyvirus CP was carried out using virus infected *Arabidopsis* leaves. Total proteins were extracted using grinding buffer (100 mM Tris HCl, 10mM KCl, 0.4 M Sucrose, 5 mM $MgCl_2$, 10% glycerol and 10mM β-mercaptoethanol) and then quantified using the Bradford assay (Bradford, 1976). Eighteen micrograms of protein were loaded onto 12% SDS-PAGE gel and then electro blotted to Amersham Hybond P 0.2 PVDF membranes (GE Healthcare Bio-Sciences, Pittsburgh, PA, USA) overnight at 200 mA. For visualization of equal protein loading, Ponceau S staining (0.5 % Ponceau S, 1 % acetic acid) was conducted (Arias Gaguancela *et al.*, 2016; Ni *et al.*, 2016). Specific capture antibodies for each virus CP was purchased from AGDIA (Elkhart, IN, USA) and used for immunoblot assay. The secondary antiserum Amersham ECL Rabbit IgG, HRP-linked whole antibody (GE Healthcare Bio-Sciences, Pittsburgh, PA, USA). Afterwards, the chemiluminescent reaction was developed using Amersham ECL Western Blotting Reagent Pack (GE Healthcare Bio-Sciences, Pittsburgh, PA, USA) and the photos of the chemiluminescent blots were taken using a 8.3 megapixel scientific – grade CCD machine (FluorChem E system - Protein Simple, San Jose, CA, USA) applying an exposure of one minute on each blot (Arias Gaguancela *et al.*, 2016).

Semi qRT-PCR and qRT-PCR assays

Semi qRT- PCR were conducted for assessment of the level of transient silencing of *bi-1* and *bzip60* genes in *N. benthamiana*. Detached leaves were harvested at 5 dpi and then subjected to RNA extraction with Maxwell 16 LEV simply RNA tissue kit (Promega Corporation, Madison, WI, USA) followed by cDNA preparation using Applied Biosystems High-Capacity cDNA Reverse Transcription Kit (Thermo Fisher Scientific Inc., Carlsbad, CA, USA). Semi qRT- PCR amplification for *bi* and *bzip60* genes were performed using GoTaq Green Master Mix (Promega Corporation, Madison, WI, USA), 10 µM dNTPs, 25 µM $MgCl_2$ and 10 µM of each sense and antisense primers (IDT- Integrated DNA Technologies, Coralville, IA, USA) described

in Table 1. Afterwards the semi qRT-PCR reactions were conducted using C1000 Touch Bio Rad thermal cycler (Bio-Rad Laboratories, Inc., Foster City, CA, USA), starting with 1 cycle at 94 °C for 10 min, followed by 35 cycles at 94 °C of denaturation for 30 s, 55 °C for annealing for 30 s and 72 °C of extension for 1.5 min, finalizing with 1 cycle at 72 °C for 10 min (Arias Gaguancela *et al.*, 2016).

qRT-PCR assays were conducted for quantification of gene expression of *bzip60 bzip28, bzip17* and *bi-1* (Table 1) and *BiP* gene candidates (Table 2) by using Kleengreen SYBR green PCR Master Mix (IBI Scientific, Peosta, IA) and 5 µM of sense and antisense primers (IDT-Integrated DNA Technologies, Coralville, IA, USA) presented in Table 1. The reactions developed in a Light Cycler 96 Real-Time System (Roche Diagnostics Corporation, Indianapolis, IN) equipment following 1 cycle of preincubation with two steps, the first one at 50 °C for 120 s and second at 95 °C for 600 s, afterwards, the amplification had 40 cycles of 60 °C for 60 s and 95 °C for 15 s, and finally 1 cycle of cooling at 37 °C for 60 s (Arias Gaguancela *et al.*, 2016).

The transcript expression levels were calculated using the comparative quantification $\Delta\Delta C_t$ method, starting with evaluating the experimental sensitivity and reproducibility with a standard curve and followed by calculation of transcript fold differences, using the following equation; **fold difference = $2^{-\Delta\Delta Ct}$**, where $\Delta\Delta C_t = \Delta C_{t\,sample} - \Delta C_{t\,reference}$, and $\Delta\textbf{C}_{\textbf{t sample}} = C_t$ of virus infected plant tissue amplified for target gene - C_t of virus infected plant tissue amplified for housekeeping or endogenous gene (*Ubiquitin* for *A. thaliana* and *Actin* for *N. benthamiana* and *S. tuberosum*). In addition, $\Delta\textbf{C}_{\textbf{t reference}} = C_t$ of plant tissue inoculated with *A. tumefaciens* without the viral construct amplified for target gene - C_t of plant tissue inoculated with *A. tumefaciens* without the viral construct amplified for housekeeping gene (Ye *et al.*, 2013; Arias Gaguancela *et al.*, 2016). For analyzing statistical differences in the gene expression of the experiments, an analysis of variance between all treatments was calculated in Relative Expression Software Tool - REST 2009, the statistical model that this program utilized was pair wise fixed reallocation which is a parametric test based on comparisons between Ct values of the samples with references with

target genes (ANOVA and Tukey methods). The proportion of how much they differ from the true mean is giving by *P*-values which is an estimate of the standard deviation (Pfaffl *et al.*, 2002).

Image J analysis

To determine the percentage of gene knockdowns or silencing for *bZIP60* and *BI-1* in *N. benthamiana* detached leaves at six dpi, the software Image J (Schneider *et al.*, 2012) was used to quantify average integrated density (AvgIntDen) from the scanned agarose gel images (16 bit .tiff format), first the images were uploaded to the program and then using the gel analyzer tool, each band present in the gel was enclosed and integrated density values (IntDen) were produced, these values represent the number of pixels present in a given area (section containing the band to analyze) multiply for the mean gray value of the background. The results were exported to Microsoft Excel - 2010 and then the percentage of gene knockdown was calculated as follows: AvgIntDen (**treated samples**; detached leaves inoculated with *A. tumefaciens* containing silencing constructs)/ AvgIntDen (**control samples**; detached leaves inoculated with *A. tumefaciens* without silencing constructs) *100 for 25, 30, and 35 cycles of amplification. For evaluating statistical differences the ratio of AvgIntDen of control samples and treated samples were paired and the standard deviation of these values resulted in probability values (*P*). If the *P* value is higher than the significance level (alpha=0.05) the null hypothesis (Ho) is accepted (silencing level is not statistically different) and on the opposite if *P* value is lower or equal than alpha, the alternative hypothesis (H1) is rejected (silencing level is statistically significant) (Arias Gaguancela *et al.*, 2016).

To analyze virus GFP on infected plant tissue, photos of the plant material were taken using Nikon D3100 DSLR camera with 18-55 mm lens and then the images were exported to Image J which selected the sections of the plant tissue presenting GFP and returned fluorescence values (FVs). FVs are equal to the Area (number of pixels per millimeter square) multiply by the

Mean gray value (sum of gray values of pixels in the section measured). FVs obtained from six plants were averaged and compared against each other. All area measurements were optimized by normalization with an internal length reference scale of 83.38 and 56.36 pixels/mm^2 for local and systemic leaves, respectively. ANOVA and Tukey methods were used to evaluate statistical differences between average FVs between wild type and mutant plants.

Table 1: List of primers used for gene expression analysis of *bZIP17*, *bZIP28*, *bZIP60* and *BI-1*.

Primer name	Sequence	Target gene	Host	Reference
Actin_F Actin_R	5'- AAA GAC CAG CTC ATC CGT GGA GAA -3' 5'- TGTGGTTTCATGAATGCCAGCAGC -3'	*Actin*	*N. benthamiana S. tuberosum*	(Zhang *et al.*, 2015)
UBQ10_F UBQ10_R	5'- GTACTTTGGCGGATTACAACATC-3' 5'- GAATACCTCCTTGTCCTGGATCT-3'	*Ubiquitin*	*A.thaliana*	(Arias Gaguancela *et al.*, 2016)
Nb-bZIP28 FWD Set1 Nb-bZIP28 REV Set1	5'-CATGGAGGCGCTGATAAGAA-3' 5'-CACTGCCGGACTTCGATAAA-3'	*bZIP28*	*N. benthamiana*	Developed in this study
Benth-bZIP17 qPCR FWD Benth-bZIP17 qPCR REV	5'-CCTATGGCTCCAATGCCTTAT-3' 5'-GGATGTTCCAAGGGTGTTCT-3'	*bZIP17*	*N. benthamiana*	Developed in this study
qPCR_AtbZIP 28 FWD Set1 qPCR_AtbZIP 28 REV Set1	5'-GAGAGATAGTTGTGGAGGAGTAGA-3' 5'-GGGACATAGAGAGAAGCAAAGAG-3'	*bZIP28*	*A.thaliana*	Developed in this study

Primer name	Sequence	Target gene	Host	Reference
AtbZIP17 FWD Set3 AtbZIP17 REV Set3	5'-CCTATGGCTCCAATGCCTTAT-3' 5'-GGATGTTCCAAGGGTGTTCT-3'	*bZIP17*	*A.thaliana*	Developed in this study
SolbZIP60_FWD SolbZIP60_REV	5'- CCTGCTTTGGTTCATGGGCATCAT-3' 5'- AGAAGACCGTGGTTTCTGCTTCGT-3'	*bZIP60*	*N. benthamiana S. tuberosum*	(Zhang *et al.*, 2015)
SolBI-1for SolBI-1rev	5'- TCCGCCAGATCTCTCCCTTT-3' 5'- AGCCACACTATGCTTCCCAC-3'	*BI-1*	*N. benthamiana S. tuberosum*	(Arias Gaguancela *et al.*, 2016)
bZIP60_FWD bZIP60-REV	5'-GCCTATTCCCTTATATGTCCCAC-3' 5'- GAACCCTTACATCTCCGACTAAC-3'	*bZIP60*	*A.thaliana*	(Moreno *et al.*, 2012)
AtBI-1_FWD AtBI_1_REV	5'- GTTAGCAAGACGCAGGGAGT-3' 5'- CTTCAAAGTGGCCACACACG-3'	*BI-1*	*A.thaliana*	(Arias Gaguancela *et al.*, 2016)
PVY-F PVY-R	5'- TGGAAGTTTGGCTCGCTATG-3' 5'- AGTCGAGATTGGGCTGATTTC-3'	PVY gRNA	*N. benthamiana*	(Arias Gaguancela *et al.*, 2016)

Table 2: list of primers used for detection of binding protein (BiP) in *A. thaliana*, *N. benthamiana* and *S. tuberosum* leaves treated with potexvirus TGB3 and potyvirus 6K2 elicitors.

Host	Primer name	Sequence	Target genes
A.thaliana	qPCR_AtBiP1/2 F qPCR_AtBiP1/2 R	5'-TCACTTGGGAGGTGAGGACTTT-3' 5'-CTCACATTCCCTTCGGAGCTTA-3'	*AtBiP1* *AtBiP2*
A.thaliana	AtBIP3- F2 AtBIP3- R2	5'-GTGGTGAAGGTGGAGAAGAAA-3' 5'-CACCGTGTTCCTCGGAATATTT-3'	*NbBiP3* *AtBiP3*
N. benthamiana	NbBLP1g022 FWD Set4 NbBLP1g022 REV Set4	5'-GCTGTCTCAATCTTCTCCTTCTC-3' 5'-TGATGCCCGTAACAGTCTTG-3'	*NtBiP1* *NtBiP2* *NbBiP1* *NbBiP2* *StBiP-D3*
N. benthamiana	NbBLP2g022 FWD Set3 NbBLP2g022 REV Set3	5'-AGACTGCCTCCACCTCTTTA-3' 5'-GTCGGATGAGAAGGAGAAGATTG-3'	*NtBiP1* *NtBiP2* *NtBiP3* *NbBiP1* *NbBiP2* *StBiP-D3*
N. benthamiana	NtBiP3 FWD Set1 NtBiP3 REV Set1	5'-GCGCTGAGAAAGAGGACTATG-3' 5'-GCTCCGCCTGATCTTTGATAA-3'	*NtBiP3* *NbBiP1* *StBiP-D3*
N. benthamiana	NtBLP4/5/8 F NtBLP4/5/8 R	5'-AAGGAGGCTGAGGAGTTTGC-3' 5'-TCAGCACTCTGGTTGTCGTC-3'	*NtBiP4* *NtBiP5* *NtBiP8*

Host	Primer name	Sequence	Target genes
			NbBiP4 *NbBiP5* *NbBiP8*
N. benthamiana	benthBIP5_00005 FWD Set benthBIP5_00005 REV Set	5'-GCTCCACTGACTCTTGGTATTG-3' 5'-GTTGTCTGCTGATCCTGGTAAG-3'	*NtBiP5* *NbBiP4* *NbBiP5* *StBiP-D5*
S. tuberosum	Potato BIP7710 qPCR FWD Potato BIP7710 qPCR REV	5'-CTCTCTTCGATGGTGTGGATTT-3' 5'-GCCTTCTTGACAGGAGTCATT-3'	*NtBiP5* *NbBiP2* *NbBiP4* *StBiP-D5*
S. tuberosum	Potato BIP1937 qPCR FWD Potato BIP1937 qPCR REV	5'-GAGGGTGGAGACGAAACTAAAG-3' 5'-GGGACTTCTTGGTTGGGATAA-3'	*NtBiP1* *NtBiP2* *NtBiP3* *NbBiP1* *NbBiP2* *StBiP-D3*
S. tuberosum	PGSC42780 FWD Set1 PGSC42780 REV Set1	5'-CTAGTGACAAGTCGCGTCTAAG-3' 5'-GAGCATCCACCTTCTCCTTTAC-3'	*SlBiP-A1* *StBiP-A2*

CHAPTER IV

RESULTS

Patterns of virus local and systemic infection in *IRE1a* and *IRE1b* defective *Arabidopsis thaliana* plants

IRE1 is a transmembrane protein that is a sensor of ER stress and malformed proteins. IRE1 leads a signaling cascade to limit accumulation of malformed proteins and maintain appropriate ER functions. *Arabidopsis* has two IRE1 proteins, IRE1a and IRE1b which are responsible for regulating *bZIP60* mRNA splicing (Chen *et al.*, 2012, 2013; Korner *et al.*, 2015). The *Potato virus X* (PVX) TGB3 or *Turnip mosaic virus* (TuMV) 6K2 proteins specifically activate *IRE1* to splice the *bZIP60* mRNA but the mechanism for IRE1 to recognize these viral proteins is not known (Ye *et al.*, 2011; Ye *et al.*, 2013; Zhang *et al.*, 2015; Arias Gaguancela *et al.*, 2016). It was undertaken investigations to characterize the roles of *IRE1a* and *IRE1b* in potexvirus (*Plantago asiatica mosaic virus*; PlAMV) and potyvirus (TuMV) infection in *Arabidopsis* plants.

It was examined whether *IRE1a* and *IRE1b* restrict PlAMV-GFP infection in inoculated leaves. Six leaves per wild-type and T-DNA tagged mutant lines *ire1a-2*, *ire1b-4* and

ire1a-2/ire1b-4 were inoculated with PlAMV-GFP. At 6 days post inoculation (dpi) leaves were detached, then photographed and subjected to Image J software analysis to quantify the average fluorescence values (FVs) across the leaf area.

The average FVs for PlAMV-GFP in mutant lines were compared with each other and the average FVs in wild-type Col-O using ANOVA. The FVs was 3- to 4- fold higher in *ire1a2* (*P*<0.01) or *ire1a-2/ire1b-4* (*P*<0.001) mutants than in wild-type Col-O leaves (Figure 1A). The FVs in *ire1b-4* mutant and Col-O leaves were not significantly different (*P*≥0.1). These data indicated that PlAMV-GFP accumulation is higher in *ire1a2* mutant plants suggesting that *IRE1a* but not *IRE1b* restricts virus movement in the inoculated leaves.

To further examine whether PlAMV-GFP infection is restricted in inoculated leaves it was used immunoblot detection to examine the levels of viral CP at 6 dpi. Immunoblot analysis revealed that the PlAMV CP accumulated to higher levels in *ire1a2* or *ire1a-2/ire1b-4* mutants than in *ire1b-4* or Col-O (Figure 1B).   These combined data indicated that knockout of *IRE1a* but not *IRE1b* leads to greater levels of PlAMV-GFP accumulation in inoculated leaves.

Next, it was examined whether virus accumulation was altered in systemically infected leaves. It was monitored the number of plants that became systemically infected over a time course of 24 dpi (Figure 2A).   It was recorded the percentage of infected 20 plants at 10 and 12 dpi (Figure 2B) and it was measured the average FVs in systemic leaves to monitor the levels of virus accumulation over the 24 day time course (Figure 2C). At 10 dpi, 40-50% of Col-O, *ire1a2* or *ire1b-4* plants were systemically infected, whereas 100% of the mutant *ire1a-2/ire1b-4* plants were infected (Figure 2B). At 12 dpi, 55% of Col-O or *ire1b-4* plants while 85% of *ire1a2* plants were systemically infected. These data suggested that knock out of the *IRE1a* gene, has a greater effect than knock out of *IRE1b* to limiting the systemic movement of PlAMV-GFP.

PlAMV-GFP was inoculated to six wild-type Col-O and mutant plants, photographed the whole plant canopy at 10, 12, 17, 19 and 24 dpi (Figure 2A), and used Image J software to obtain the average FVs as a measure of systemic virus accumulation. The average FVs were plotted over time and compared using ANOVA. The average FVs were significantly higher in *ire1a2* (*P*<0.05) or *ire1a-2/ire1b-4* (*P*<0.01) than Col-O. PlAMV-GFP accumulation in wild-type Col-O and *ire1b-4* mutant plants were similar (*P*≥0.1; Figure 2C). These combined data indicated that *IRE1a* plays a greater role in PlAMV-GFP infection than *IRE1b*.

Similar experiments were carried out using the TuMV-GFP infectious clone provided by Dr. Aiming Wang (Southern Crop Protection and Food Research Center) to examine if *IRE1a* and/or *IRE1b* plays a role in virus accumulation. In the inoculated leaves, the average FVs were 4- to 5- fold higher in *ire1a2* (*P*<0.05) and *ire1b-4* (*P*<0.01) mutant leaves than Col-O leaves. The average FVs in *ire1a-2/ire1b-4* double mutant lines (*P*<0.001) was 6-fold greater than in Col-O leaves (Figure 1C). The immunoblot analysis revealed that TuMV CP was higher in *ire1a2, ire1b-4* or *ire1a-2/ire1b-4* than in Col-O leaves (Figure 1D). These data indicated that *IRE1a* and *IRE1b* comparably influence TuMV-GFP accumulation in inoculated leaves. There did not appear to be a preferred dependence upon *IRE1a* as for PlAMV-GFP.

Next, it was examined TuMV-GFP accumulation in systemically infected leaves. It was monitored the number of plants that became systemically infected over a time course of 24 dpi (Figure 3A). It was recorded the percentage of infected 18 plants at 10 and 17dpi (Figure 3B) and it was measured the average FVs in systemic leaves to monitor the levels of virus accumulation over the 24 day time course (Figure 3C). At 10 dpi, 0% of wild-type Col-O were systemically infected whereas 44% of *ire1a*, and 100% of *ire1b-4* and *ire1a-2/ire1b-4* plants were systemically infected (Figure 3B). At 17 dpi, approximately 50% of Col-O plants were systemically and 100% of *ire1a2, ire1b-4* and *ire1a-2/ire1b-4*plants were systemically infected (Figure 3B). The average FVs in six TuMV-GFP systemically infected plants were obtain at 10,

12, 17, 19 and 24 dpi. TuMV-GFP accumulated to higher levels in *ire1b-4* (*P*<0.05) and *ire1a-2/ire1b-4* (*P*<0.01) than Col-O. TuMV-GFP accumulation was not significantly different among *ire1a-2* and wild-type Col-O plants (*P*≥0.1; Figure 3C). These data indicated that *IRE1b* has a greater role in restricting TuMV-GFP systemic accumulation than *IRE1a*.

These data indicated that *IRE1a* restricts PlAMV-GFP movement in both local and systemic plants tissues. *IRE1a* might participated in recognition of PlAMV TGB3. In the case of TuMV-GFP infection, virus restriction was equally affected by mutations in either *IRE1a* or *IRE1b* in inoculated leaves but *IRE1b* played a greater role in restricting systemic accumulation. These results suggested that both *IRE1* genes might participate in recognition of TuMV 6K2.

A)

Col-O | ire1a-2 | ire1b-4 | 1a/b

FV: 1 5 1 4

B)

C(-) 1b 1a C | C(-) 1a/b C

C)

Col-O | ire1a-2 | ire1b-4 | 1a/b

FV: 1 4 5 6

D)

1b 1a Col-O | Col-O 1a/b C(-)
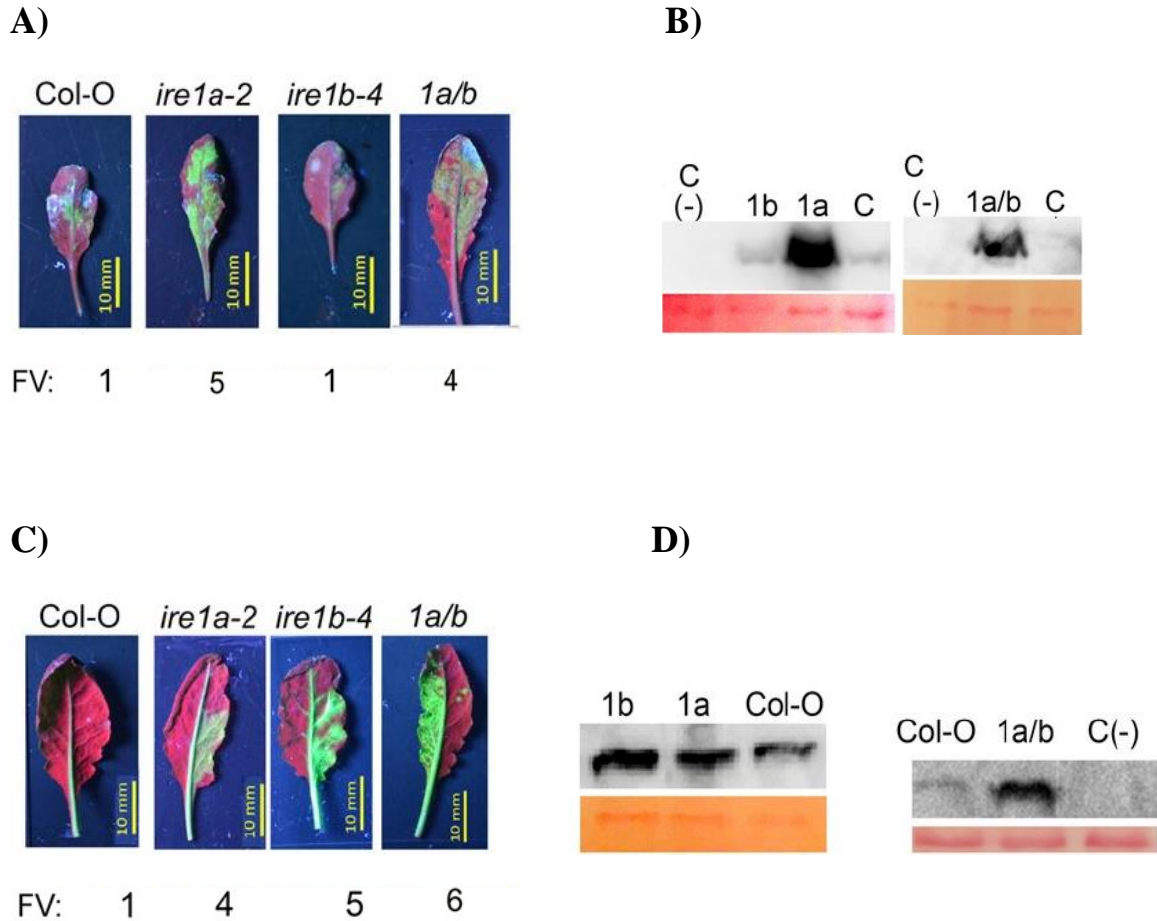
Figure 1: PlAMV-GFP and TuMV-GFP infecting local leaves of *Arabidopsis* plants. (A) and (C) show representative images of PlAMV-GFP and TuMV-GFP inoculated leaves at 6 days post inoculation (dpi). Fold of increase of average fluorescence values (FVs) for each mutant line with respect to Col-O are written below each photo. Each photo was taken under UV light. Healthy leaves auto fluorescence red under UV light, while green fluorescence shows the pattern of PlAMV-GFP or TuMV-GFP fluorescence. (B) and (D), Immunoblots detected viral CP in PlAMV-GFP and TuMV-GFP inoculated leaves. Lane 1b is *ire1b-4*, lane 1a is *ire1a-2*, lane 1a/b is *ire1a-2/ire1b-4* mutant, lane C is Col-O and lane C (-) corresponds to healthy control. Ponceau S staining below immunoblots show equal loading of ribosomal protein in each well.
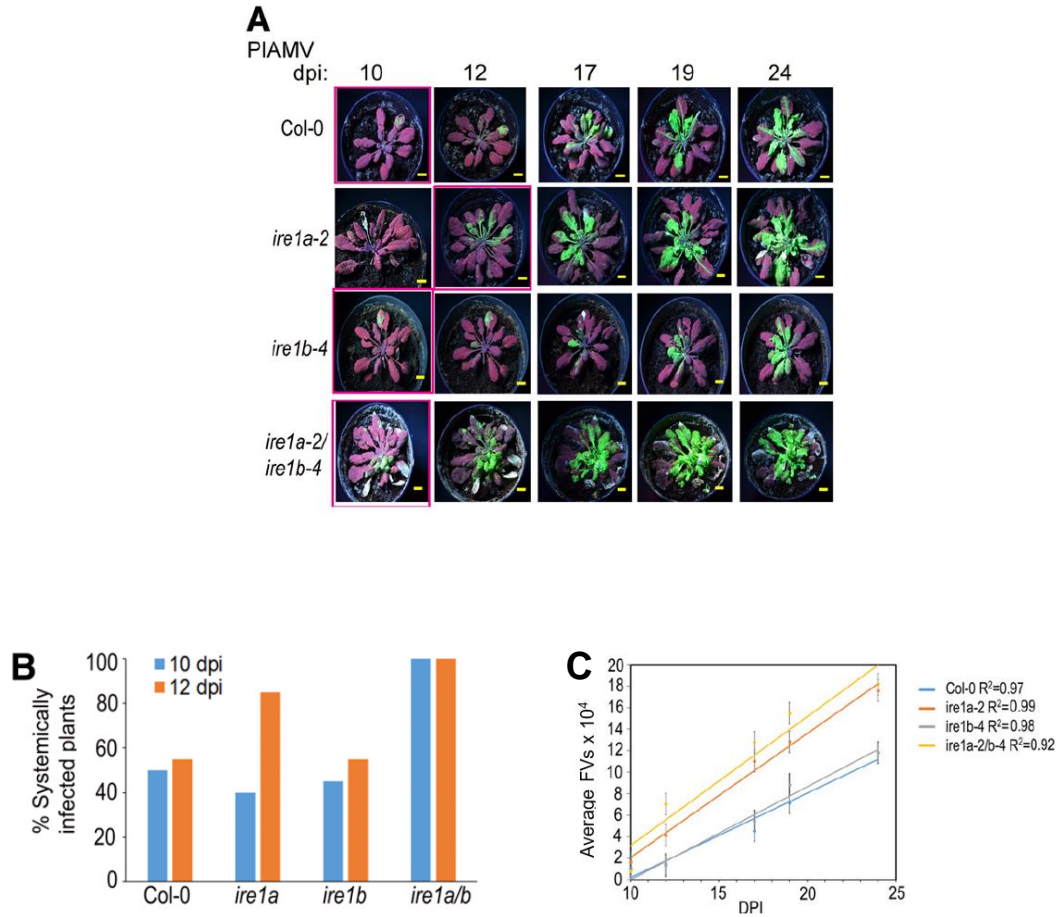
Figure 2: PlAMV-GFP infecting systemic tissues of *IRE1* mutant *Arabidopsis* plants. (A)
Representative images of PlAMV-GFP systemic infected *Arabidopsis* wild-type, *ire1a-2*, *ire1b-4*
and *ire1a-2/ire1b-4* mutant lines taken between 10 and 24 days post inoculation (dpi). Photos
were taken with a UV lamp. Leaves auto fluorescence red under UV light, while green
fluorescence shows the pattern of PlAMV-GFP fluorescence. Red squares around the photo
outlines the first day that systemic infection was first observed. (B) Percent of systemically
infected plants at 10 or 12 dpi calculated from 20 plants per wild-type and mutant line. (C)
Graphical representation of the average fluorescence values (FVs) in PlAMV-GFP infected
systemic leaves (six plants per wild-type and mutant line) recorded at 10, 12, 17, 19 and 24 dpi.
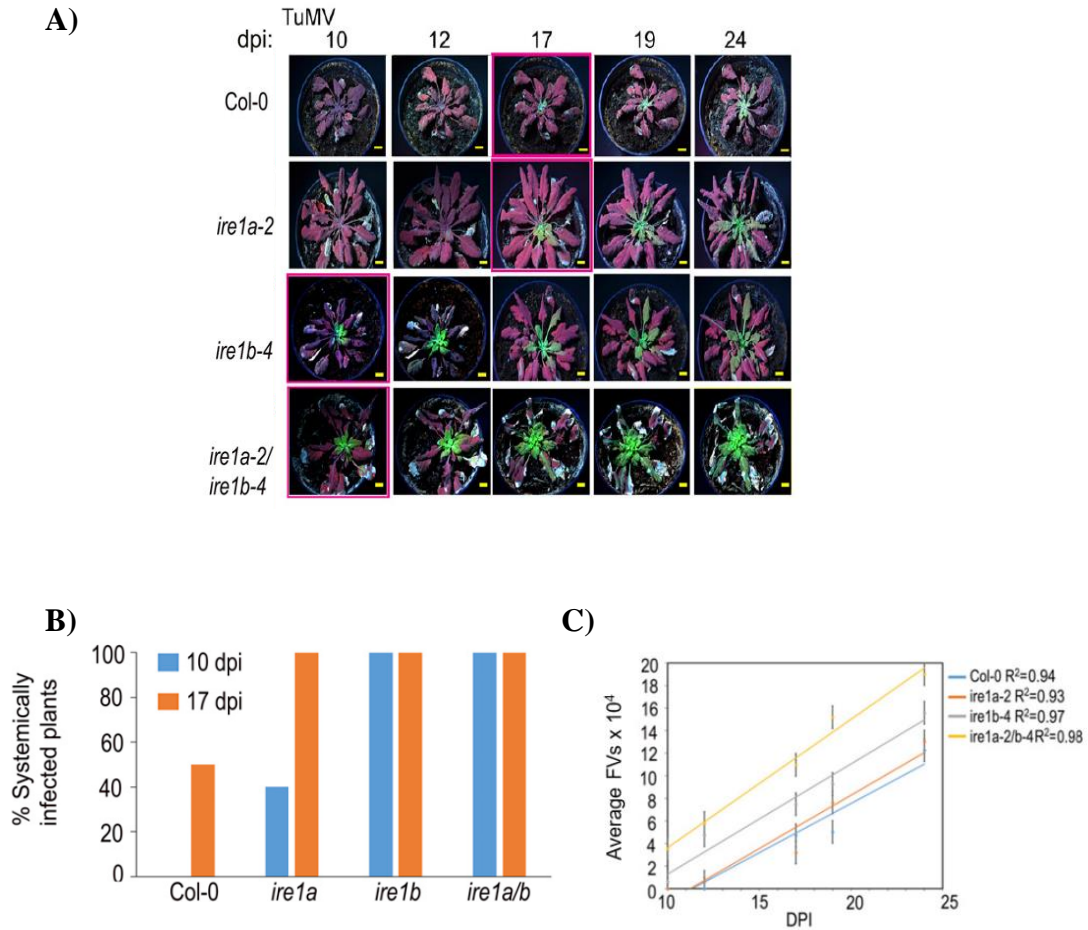
Figure 3: TuMV-GFP systemically infected wild type and *IRE1* mutant *Arabidopsis* plants. (A) Representative images of TuMV-GFP systemically infected *Arabidopsis* between 10 and 24 days post inoculation (dpi); wild type, *ire1a-2*, *ire1b-4* and *ire1a-2/ire1b-4* mutant lines. Photos were taken with a UV lamp. (B) Percent of systemically infected plants at 10 or 17 dpi calculated from 18 plants per wild-type and mutant line (C) Graph of the average fluorescence values (FVs) (six plants per wild-type and mutant line) represent TuMV-GFP accumulation recorded at 10, 12, 17, 19 and 24 dpi.

qRT-PCR analysis of *bZIP60, bZIP17* and *bZIP28* induction following treatment with viral elicitors

      bZIP17, bZIP28 and *bZIP60* are transcription factors tethered to the ER. Activation of bZIP60 is dependent upon IRE1 splicing the *bZIP60* mRNA to remove the transmembrane encoding domain. Project collaborator Dr Aiming Wang previously showed that *bZIP60* expression is upregulated following delivery of the PVX TGB3 or TuMV 6K2 genes (Ye *et al.*, 2011; Ye *et al.*, 2013; Zhang *et al.*, 2015). It was used qRT-PCR to learn if *bZIP17* or *bZIP28* transcripts were elevated following agro-delivery of PlAMV TGB3, PVX TGB3, TuMV 6K2 or PVY 6K2 to *Arabidopsis* (Col-O ecotype) and *N. benthamiana* leaves. Control leaves were treated with *Agrobacterium* only.

      qRT-PCR assays were performed using RNA extracted from inoculated leaves at 2 and 5 days post inoculation to observe changes in the levels of *bZIP17, bZIP28,* and *bZIP60* transcripts (Figure 4A).   At 2 dpi, the level of *bZIP60* transcripts in PVX TGB3 or PVY 6K2 infiltrated *Arabidopsis* Col-O leaves was 2.6-fold above the control ($P<0.05$) and there was no change in *bZIP60* transcripts following delivery of PlAMV TGB3 or TuMV 6K2 ($P<0.05$). There was no change in *bZIP17* and *bZIP28* transcript accumulation in *Arabidopsis* leaves following delivery of PlAMV TGB3, PVX TGB3, TuMV 6K2 or PVY 6K2 ($P<0.05$; Figure 4A).

      qRT-PCR assays were performed at 5 dpi and the level of *bZIP17* transcripts was ~2-fold above the control following agro-delivery of the PlAMV TGB3, TuMV 6K2 or PVY 6K2 ($P<0.05$) but not PVX TGB3 genes ($P<0.05$). For *bZIP28,* an average transcript level was ~2-fold above the control following agro-delivery of TuMV 6K2 or PVY 6K2 ($P<0.05$) but not PlAMV TGB3 or PVX TGB3 ($P\geq0.01$; Figure 4A). *bZIP60* transcript level was between 2.4 and 3.6- fold above the control following agro-delivery of TuMV 6K2 or PVY 6K2 ($P<0.05$) but not following agro-delivery of PlAMV TGB3 or PVX TGB3 ($P\geq0.01$; Figure 4A). The two potyvirus 6K2

genes appeared to induce expression of *bZIP60*, *bZIP17* and *bZIP28* at either 2 or 5 dpi. The two potexvirus TGB3 genes appeared to induce either *bZIP60* or *bZIP17* at 2 or 5 dpi.

Next, qRT-PCR assays were performed using RNA extracted from *N. benthamiana* leaves following agro-delivery of these four virus genes (Figure 4B). At 2 dpi following agro-delivery of PlAMV TGB3, PVX TGB3, TuMV 6K2 or PVY 6K2 genes, there was no change in the levels of *bZIP17* transcripts ($P<0.05$), whereas *bZIP28* was elevated 2.3- to 3- fold and *bZIP60* was elevated 6.6- to 11.3- fold ($P<0.05$; Figure 4B). At 5 dpi, *bZIP17* transcripts were 3.2 to 4- fold following agro-delivery of PVX TGB3 or PVY 6K2. *bZIP28* transcripts were elevated by 2.8 to 5-fold following agro-delivery of PlAMV TGB3, PVX TGB3, TuMV 6K2 or PVY 6K2 genes above the control ($P<0.05$). The *bZIP60* average transcript was 2.3-fold following agro-delivery of PVX TGB3 ($P<0.05$) but not following agro-delivery of PlAMV TGB3, TuMV 6K2 or PVY 6K2 genes ($P\geq0.05$; Figure 4B). These data obtained in *N. benthamiana* plants indicated that the four viral proteins induce *bZIP60* and *bZIP28* and two viral proteins appeared to activate *bZIP17*. In both *Arabidopsis* and *N. benthamiana*, the transcript levels for each gene changed, however the timing and levels of transcript accumulation in *N. benthamiana* was somewhat different than in *Arabidopsis*.

A)

B)
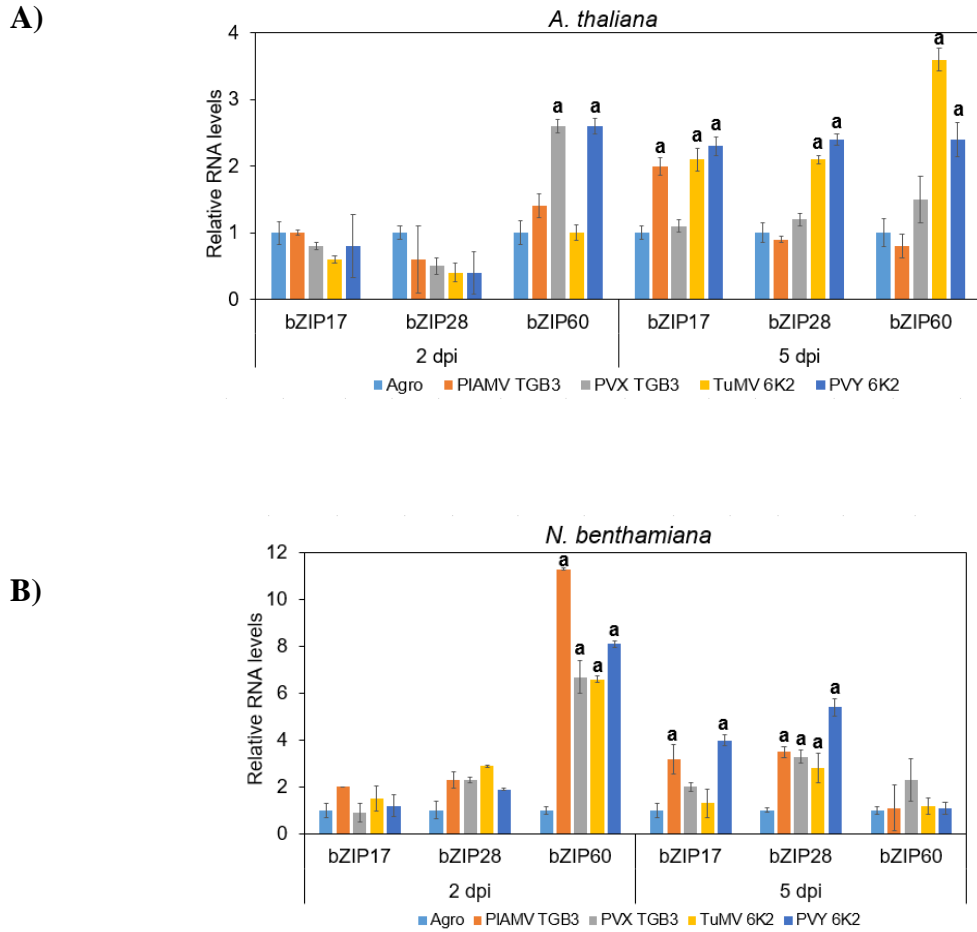
Figure 4: Results of qRT-PCR detecting *bZIP17*, *bZIP28* and *bZIP60* in *Arabidopsis* Col-O (A) and *N. benthamiana* (B) leaves at 2 and 5 days post inoculation (dpi). Key below graphs identify bars corresponding to each viral elicitor treatment. Control leaves were infiltrated with *Agrobacterium* (Agro) that does not deliver a viral gene. Each colored bar is an average of three independently infiltrated leaves. Error bars represent the level of standard deviation in each treatment. ANOVA and Tukey methods were used for evaluating statistical differences. Bars that were statically different from the control were identified with the letter "a" for a significance level of ($P<0.05$).

Patterns of virus local and systemic infection in *bZIP17, bZIP28* and *bZIP60* defective *Arabidopsis* plants

It was investigated PlAMV-GFP accumulation in inoculated and systemically infected leaves of wild-type Col-O and *bzip17*, *bzip28* and *bzip60, bzip17/bzip60, and bzip28/bzip60* plants. Evelyn Vasquez, a visiting scholar at OSU (Department of Entomology of Plant Pathology) was in charge of agro-inoculating and monitoring the patterns of infection in these plants. I performed the (photography) and Image J analysis to obtain average FVs. The average FVs compared using ANOVA to determine if knock down of these genes altered the accumulation of PlAMV-GFP.

The average FVs in PlAMV-GFP inoculated leaves were calculated for six leaves of wild-type or mutant *Arabidopsis* plants at 5 dpi (Figure 5A). In *bzip17, bzip60,* or *bzip17/bzip60* inoculated leaves, the average FVs were 7- to 9- fold higher than Col-O infected leaves (*P*<0.001). For *bzip28*, *bzip28/bzip60* mutant plants, the average FVs were ~2- to 3- fold greater than Col-O infected leaves (Figure 5A). These data showed that in *Arabidopsis bZIP17* or *bZIP60* have a greater role in restricting PlAMV-GFP accumulation in local leaves.

Arabidopsis plants that were systemically infected with PlAMV-GFP were photographed at 10, 12, 17 and 19 dpi, using a six plants per wild-type and mutant line. The average FVs were determined using Image J software analysis as in prior experiments involving *IRE1*-defective plants (Figure 6A). Statistical analysis of the trend lines indicated that the average FVs were higher in *bzip17, bzip60 or bzip17/bzip60* mutant plants than in wild-type Col-O plants (*P*<0.001; Figure 6B). At 19 dpi the average FVs for PlAMV-GFP in the *bzip17/bzip60* mutant plants was ~60 x 10^3 FVs, in *bzip17* mutant plants was 31 x 10^3 FVs and in *bzip60* was 57 x 10^3 FVs (Figure 6B). The trend lines for PlAMV-GFP systemic accumulation in *bzip28* and *bzip28/bzip60* was different from all other plants (*P*<0.005) (Figure 6B). At 19 dpi the average FVs in *bzip28* mutants was 17.4 x 10^3 FV and in *bzip28/bzip60* mutant plants was 13.2 x 10^3 FVs (Figure 6B).

The average FVs in wild-type Col-O at 19 dpi was 8.4 x 10^3 FVs. These data demonstrated that knocking out *bZIP17* and/or *bZIP60* expression led to higher levels of systemic PlAMV-GFP accumulation than in wild-type or *bzip28* knock out plants. Importantly knocking out *bZIP28* also led to greater accumulation of PlAMV-GFP, but not to the same extent as *bZIP17* or *bZIP60* mutations.

TuMV-GFP was inoculated in the same wild-type and mutant plants to examine whether *bZIP17, bZIP28* or *bZIP60* play a role in virus restriction in inoculated leaves and systemic plants. FVs were measured in a six inoculated leaves per wild-type and mutant line at 8 dpi (Figure 5B). The FVs in the inoculated leaves of *bzip28* ($P<0.01$) or *bzip60* ($P<0.05$) mutant plants were 3- fold higher than in wild-type Col-O plants. The average FVs for TuMV-GFP accumulation in the inoculated leaves of *bzip17* or *bzip17/bzip60* mutants plants and wild-type Col-O plants were not significantly different ($P\geq0.1$; Figure 5B). These data suggested that *bZIP28* and *bZIP60* restrict TuMV-GFP infection.

TuMV-GFP systemically infected *Arabidopsis* plants were photographed at 10, 12, 17 and 19 dpi. The average FVs in six plants per wild-type and mutant line were calculated and plotted as in prior experiments involving IRE1 mutant plants (Figure 7A). Statistical analysis of the trend lines indicated that the average FVs were higher in *bzip28, bzip60, bzip17/bzip60 and bzip28/60* mutant plants than in Col-O wild-type plants ($P<0.001$; Figure 7B). The trend lines for *bzip*17 and Col-O wild-type plants were not significantly different ($P\geq0.05$; Figure 7B). In a lower scale, *bzip28, bzip60* and *bzip17* accumulated TuMV-GFP in a greater level than Col-O wild-type plants ($P<0.001$). These data indicated that knocking out *bZIP28*, *bZIP60* or the combined genes leads to greater systemic accumulation of TuMV-GFP.

A)

B)
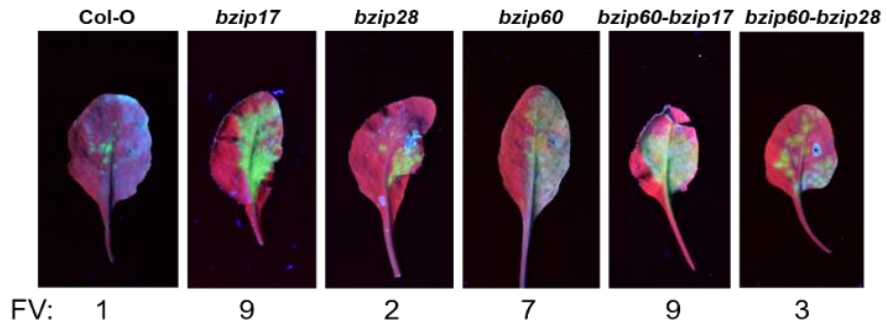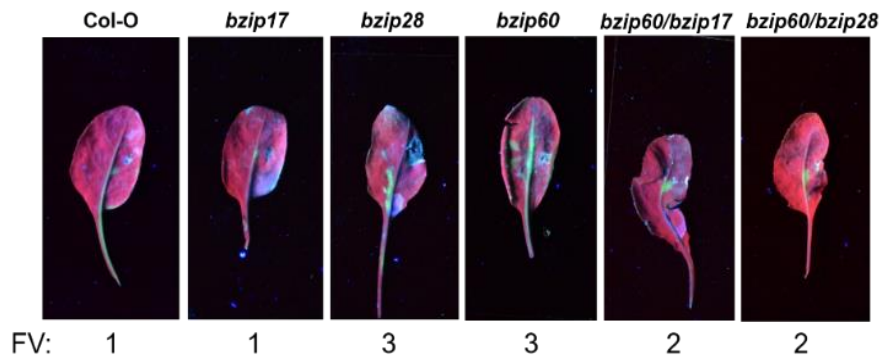
Figure 5: PlAMV-GFP and TuMV-GFP infecting local leaves of wild-type Col-O, *bzip17*, *bzip28*, *bzip60*, *bzip60/bzip17* and *bzip60/bzip28 Arabidopsis* mutant lines. (A) and (B) show representative images of PlAMV-GFP and TuMV-GFP inoculated leaves at 5 and 8 days post infiltration (dpi), respectively. Fold of average fluorescence values (FVs) of each plant line respect to Col-O are written below each photo. Each photo was taken under UV light.
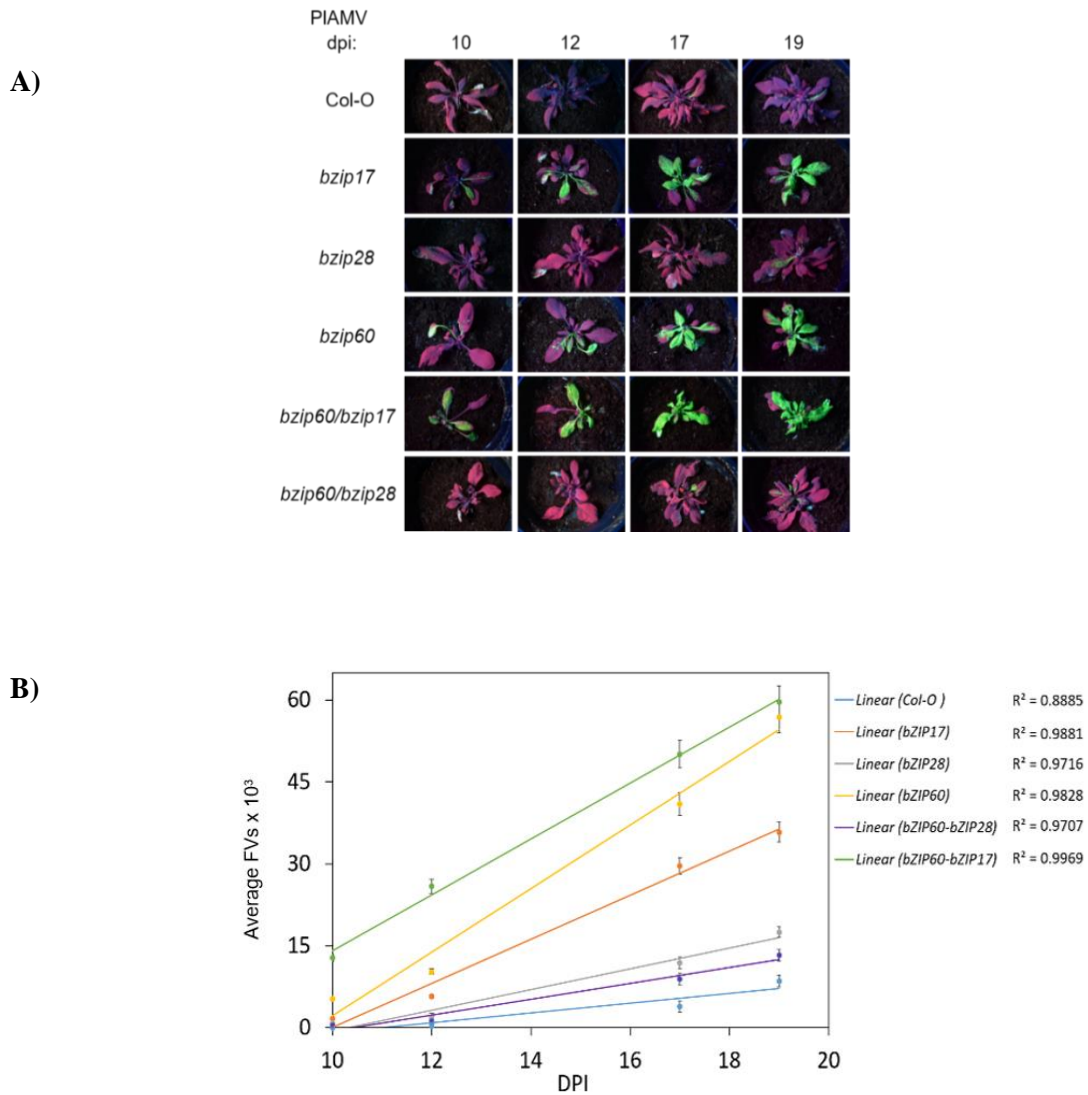
Figure 6: PlAMV-GFP infecting systemic tissues of *Arabidopsis* plants. (A) shows a sequence of representative images representing the progress of PlAMV-GFP systemic infection in wilt-type Col-O, *bzip17*, *bzip28*, *bzip60*, *bzip60/bzip17* and *bzip60/bzip28* mutant lines from 10 to 19 days post infiltration (dpi). Photos were taken with a UV lamp. (B), trend line graph of average fluorescence values (FVs) represent the level of PlAMV-GFP accumulation in the systemic tissues of six *Arabidopsis* plants recorded at 10, 12, 17 and 19 dpi.

A)

B)
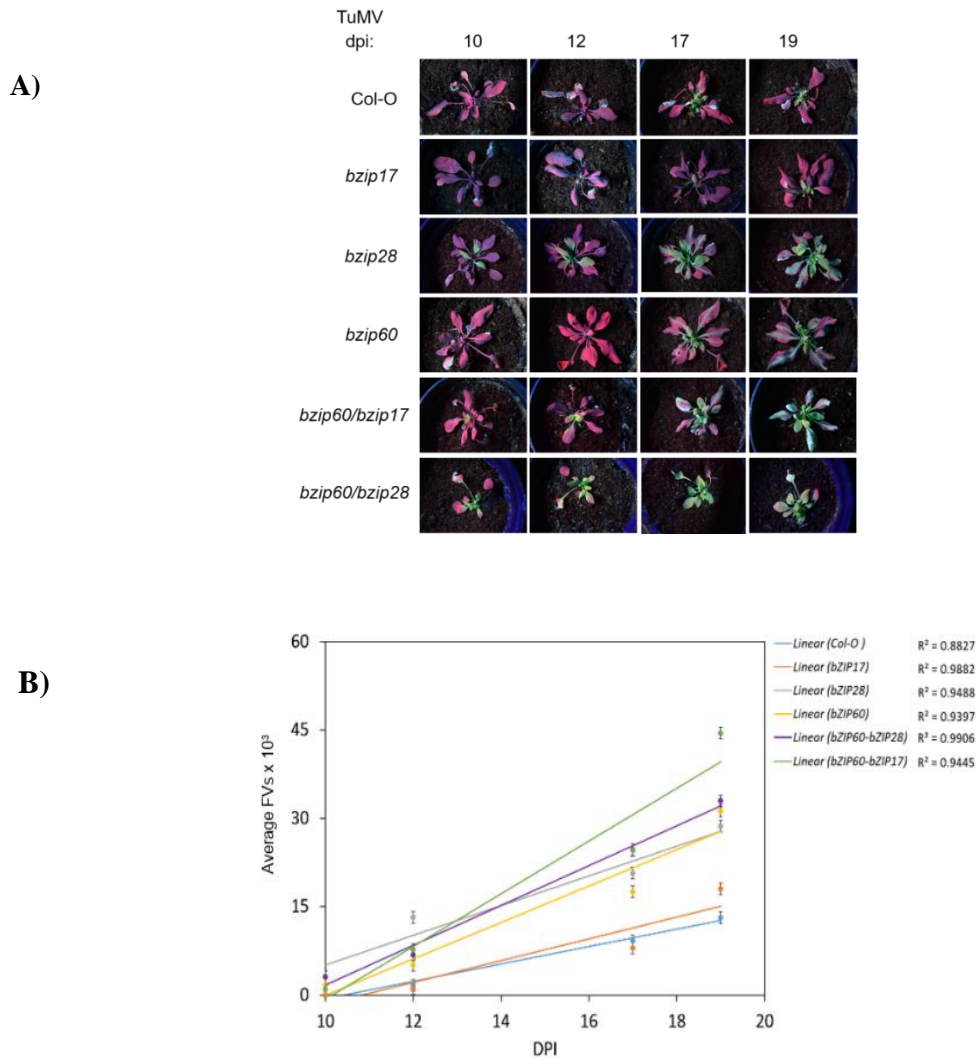
Figure 7: TuMV-GFP infecting systemic tissues of *Arabidopsis* plants. Section (A) shows a sequence of representative images representing the progress of TuMV-GFP systemic infection in wilt-type Col-O, *bzip17*, *bzip28*, *bzip60*, *bzip60/bzip17* and *bzip60/bzip28* mutant lines from 10 to 19 days post infiltration (dpi). Photos were taken with a UV lamp. (B), trend line graph of average fluorescence values (FVs) represent the level of PlAMV-GFP accumulation in the systemic tissues of six *Arabidopsis* plants recorded at 10, 12, 17 and 19 dpi.

qRT-PCR analysis of ER luminal binding protein (BiP) gene expression following treatment with viral elicitors

The ER luminal binding protein (BiP) belongs to a family of hsp70 chaperones and its expression can be induced by the transcription factors *bZIP60*, *bZIP28*, and *bZIP17*. BiP is a master regulator in the ER lumen involved in protein translocation and protein folding and is linked with protection against several forms of abiotic and biotic stress (Carolino *et al.*, 2003; Carvalho *et al.*, 2014). Dr Verchot's laboratory reported that *BiP* gene expression increases following agro-deliver of the PVX TGB3 or following PVX-GFP inoculation to *N. benthamiana* plants (Ye *et al.*, 2011; Ye *et al.*, 2013). Each plant species has several copies of *BiP* genes. In *Arabidopsis* plants there are *AtBiP1*, *AtBiP2* and *AtBiP3*. In *N. benthamiana*, there are *NbBiP1*, *NbBiP2*, *NbBiP3*, *NbBiP4/5/8* and *NbBiP5*. Dr Dennis Halterman (USDA-ARS) used the SPUD database (Potato Genomics Resource) to identify candidate *BiPs* in *S. tuberosum* and Dr Verchot used these sequences to conduct phylogenetic analysis to relate these genes to those in *Arabidopsis* and *N. benthamiana, N. tabacum* and potato. Dr Halterman identified three *BiP* candidate genes recognized by the accessions numbers: PGSC003DMP400042780, PGSC0003DMT400031937, and PGSC003DMT400047710. For the purposes of this study, they were named as *StBiP-A-2*, *StBiP-D3*, and *StBiP-D5*, respectively.

It was performed qRT-PCR assays to determine if *BiP* gene expression in *Arabidopsis*, *N. benthamiana* increases following agro-delivery of the PlAMV TGB3, PVX TGB3, TuMV 6K2 or PVY 6K2 genes. In *S. tuberosum*, *BiP* gene expression was measured following agro-delivery of PVX TGB3 or PVY6K2. Control leaves were treated with *Agrobacterium* only. RNA was extracted from the inoculated leaves at 2 and 5 days from *Arabidopsis* and at 2 days from *N. benthamiana* and *S. tuberosum* leaves. RNA was used for the qRT-PCR assays.

It was used two sets of qRT-PCR primers for detecting *Arabidopsis* genes (Figure 8A, Table 2). *AtBiP1* and *AtBiP2* have 99% similarity therefore one set of PCR primers (*AtBiP1/2*)

detect both genes. A second set of primers detect *AtBiP3* only. With regard to the combined *AtBiP1* and *AtBiP2* transcripts, there was no variation in transcript accumulation following delivery of any viral elicitor at 2 dpi. At 5 dpi, the average level of the combined *AtBiP1* and *AtBiP2* was elevated ~2-fold above the average level in control leaves following agro-delivery of TuMV 6K2 or PVY 6K2 but not PlAMV TGB3 or PVX TGB3. Increased *AtBIP1/2* accumulation was a specific response to the potyvirus 6K2 gene ($P<0.05$; Figure 8A).

With regard to *AtBiP3* transcripts, the average level at 2 dpi was ~2- fold higher in leaves following agro-delivery of PVX TGB3 compared to control leaves, but there was no variation in the average levels following delivery of PlAMV TGB3, TuMV 6K2 or PVY 6K2. At 5 dpi following agro-delivery of PVX TGB3, PlAMV TGB3, TuMV 6K2 or PVY 6K2 , the average levels of *AtBiP3* transcripts increased to levels between 2.5- and 3.9- fold above the control ($P<0.05$; Figure 8A).

Five sets of qRT-PCR primers were used for detecting *N. benthamiana BiP* transcripts (Figure 8B, Table 2) and all data was collected at 2 dpi. Four sets of PCR primers were generated to distinguish *NbBiP1*, *NbBiP2, NbBiP3, and NbBiP5* transcripts. Another primer set named NbBIP4/5/8 detects the combined *NbBiP4, NbBiP5,* and *NbBiP8* transcripts. The average levels of *NbBiP1* and *NbBiP2* transcripts following agro-delivery of PVX TGB3, PlAMV TGB3, TuMV 6K2, or PVY 6K2, were ~3 to 6- fold above the control ($P<0.05$; Figure 8B). Interestingly, the average levels of *NbBiP3* transcripts were 7.7 to 10- fold following agro-delivery of PVX TGB3, PlAMV TGB3, TuMV 6K2, or PVY 6K2 ($P<0.05$). The average levels of the combined *NbBiP4/5/8* transcript fell into two categories. For PVX TGB3 and PVY 6K2 treated leaves, the combined transcripts were highly elevated, 17.1 and 13.5- fold over the control, respectively ($P<0.001$). For PlAMV TGB3 and TuMV 6K2 the combined transcripts were elevated to 6.1 and 3.1-fold above the controls, respectively ($P<0.05$). Using *NbBiP5* specific primer set, the average levels were 20.7 and 16.6- fold over the control following agro-

delivery of PVY 6K2 and PVX TGB3 (*P*<0.001). The average levels of *NbBIP5* transcripts were 9.6 and 6.1- fold above the control following agro-delivery of PlAMV TGB3 and TuMV 6K2, respectively (*P*<0.05; Figure 8B). In *N. benthamiana* the transcript levels for each *BiP* candidate was elevated. Notably the combined detection of *NbBiP4, NbBiP5,* and *NbBiP8* transcripts, which are not related phylogenetically to *AtBiP1, AtBiP2, or AtBiP3* responded most dramatically to the viral elicitors.

In *S. tuberosum*, three primer sets were used to detect *StBiP-A*, *StBiP-D3*, and *StBiP-D5* candidate genes identified by Dr. Halterman. All qRT-PCR assays were conducted at 2 dpi. The average levels of *StBiP-D3* and *StBiP-D5* transcripts following agro-delivery of PVX TGB3 and PVY 6K2, were ~2.3 and 3.1 fold above the control (*P*<0.05; Figure 8C). With regard to *StBiP-A* transcripts, there was no variation in transcript accumulation following delivery of any viral elicitor. These genes are phylogenetically distinct from the *Arabidopsis AtBiP1, AtBiP2, or AtBiP3* genes.

A)

B)

C)
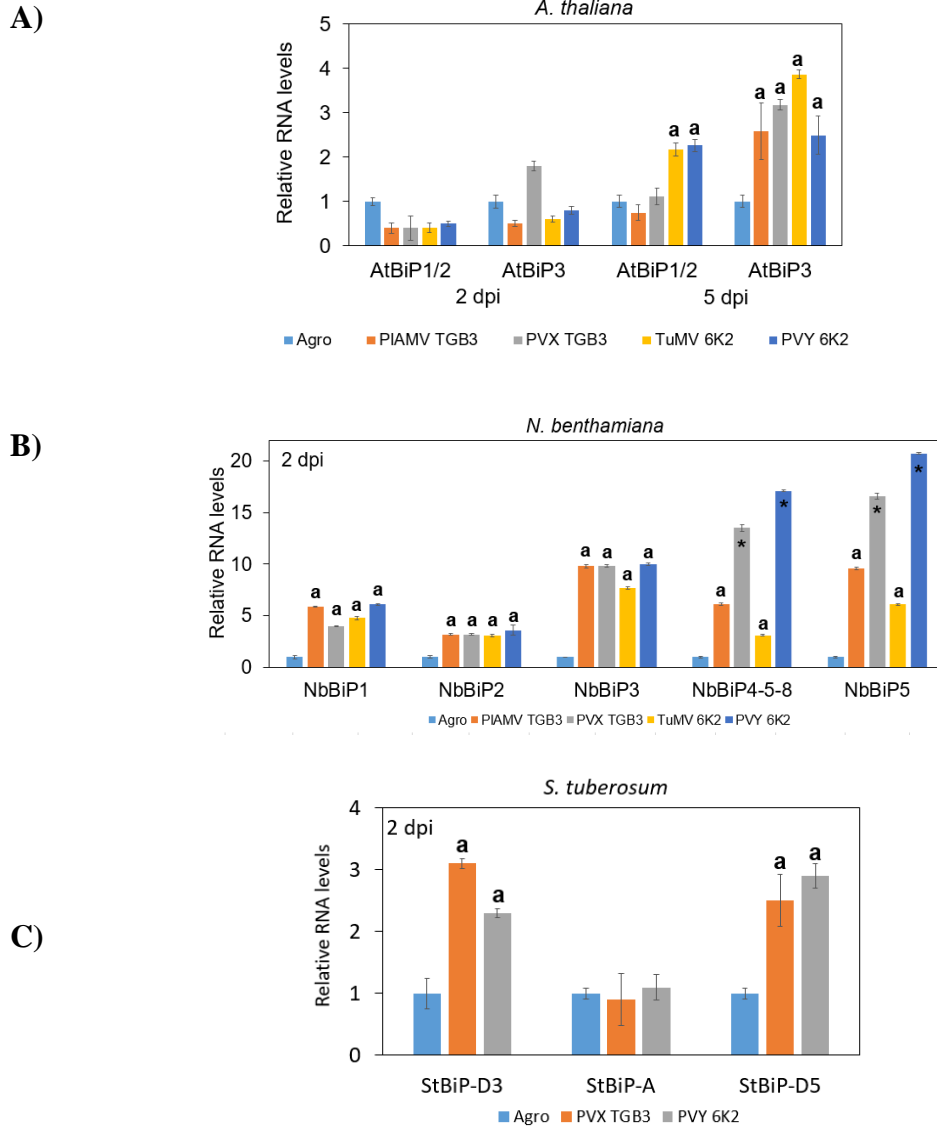
Figure 8: Results of qRT-PCR detecting *BiP* genes in detached leaves from *Arabidopsis* (A) and *N. benthamiana* (B) and (C) *S. tuberosum* inoculated with TGB3 potexvirus or potyvirus 6K2. Key below graphs identify bars corresponding to each viral elicitor treatment. Control leaves were infiltrated with *Agrobacterium* (Agro) that does not deliver a viral gene. Error bars represent the level of standard deviation in each treatment. ANOVA and Tukey methods were used for evaluating statistical differences. Bars that were statically different from the other colored bars were identified with the letter "a" or an asterisk "*" for significance levels of ($P<0.05$) and ($P<0.001$), respectively.

Comparison of the patterns of local and systemic PlAMV-GFP and TuMV-GFP infection in

***BI-1*, *IRE1a/IRE1b* and *bZIP60* defective *Arabidopsis* plants**

BI-1 is a cell death suppressor that resides in the ER. It was hypothesized that *BI-1* expression was controlled by *IRE1* and *bZIP60* based on reports from (Lisbona *et al.*, 2009; Ishikawa *et al.*, 2011b). To test this hypothesis, my colleague Liz Peña conducted qRT-PCR assays to determine if *BI-1* expression was altered in *ire1a-2/ire1b-4* and wild-type *Arabidopsis* plants. Based on her results it was not possible to conclude that there was any pattern of gene expression linking *BI-1* to *IRE1a, IRE1b* or *bZIP60*. In this study, plants that were defective for *bi-1*, *ire1a-2/ire1b-4*, and *bzip60* were inoculated with PlAMV-GFP or TuMV-GFP to determine if these genes similarly impact the ability of each virus to spread locally and systemically. If *BI*-1 were downstream of *IRE1* or *bZIP60,* the timing of infection and the accumulation of GFP and CP would be comparable in mutant lines. If *BI-1* was independent of *IRE1* or bZIP60, GFP and CP accumulation would be unique.

The FVs for PlAMV-GFP in *bi-1*, *irea1a-2/ire1b-4*, *bzip60* mutant and wild-type Col-O plants were examined and compared. Six leaves per wild-type and T-DNA tagged mutant lines were inoculated with PlAMV-GFP. At 6 dpi, the average FVs for PlAMV-GFP accumulation in mutant lines were compared with each other and the average FVs in wild-type Col-O using ANOVA. The average FVs showed that PlAMV-GFP accumulation was 3 to 4- fold higher in *bi-1, irea1a-2/ire1b-4,* and *bzip60* mutant plants than in Col-O wild-type leaves ($P<0.001$; Figure 9A). *BI-1, IRE1a, IRE1b,* and *bZIP60* similarly restricted PlAMV-GFP accumulation.

To further examine whether virus infection is restricted in inoculated leaves, immunoblot detection was used to examine the levels of viral CP in *BI-1* or *bZIP60* leaves at 6 dpi. Immunoblot analysis revealed that PlAMV CP accumulated to higher levels in *BI-1* or *bZIP60* than in wild-type Col-O leaves (Figure 9B). These data indicated that *BI-1, IRE1,* and *bZIP60* comparably influence PlAMV-GFP accumulation in inoculated leaves.

Next, it was examined whether virus accumulation was altered in systemically infected leaves. The number of plants that became systemically infected were monitored over a time course of 24 dpi (Figure 10A). The percentage of 20 systemically infected plants were observed at 10 and 12 dpi (Figure 10B) and the average FVs were measured in systemic leaves to monitor the levels of virus accumulation over the 24 day time course (Figure 10C). At 10 dpi, between 45% and 50% of wild type Col-O and *bzip60* plants were systemically infected whereas 100% of *bi-1* mutant lines were systemically infected. At 12 dpi, systemic infection reached 50 to 80% for Col-O and *bzip60* plants (Figure 10B). PlAMV-GFP was inoculated to six wild-type Col-O and mutant plants, photographed the whole plant canopy at 10, 12, 17, 19 and 24 dpi (Figure 10A), and used Image J software to obtain the average FVs . The average FVs were plotted over time and compared using ANOVA. PlAMV-GFP accumulate to higher levels in *bi-1* mutant lines than in *ire1a-2/ire1b-4, bzip60* and in Col-O wild-type plants (*P*<0.05; Figure 10C). These data indicated that *bi-1* has a greater role in restricting systemic PlAMV-GFP accumulation than *ire1a-2/ire1b-4* or *bzip60.* Thus suggesting that *BI-1* might not be involved in regulating events upstream of *IRE1* or *bZIP60* expression.

Similar experiments were carried out using the TuMV-GFP infectious clone provided by Dr. Aiming Wang (Southern Crop Protection and Food Research Center). In the inoculated leaves, the average FVs values in *bi-1* mutant plants were 11-fold greater than Col-O. TuMV-GFP accumulation in *irea1a-2/ire1b-4* and *bzip60* mutant plants (*P*<0.01) was 3- and 5-fold greater than wild-type Col-O leaves. The immunoblot analysis revealed that the levels TuMV CP were similar in wild-type and mutant lines. Bases on the FVs data, it seemed that *BI-1* might played a greater role in TuMV-GFP infection than *IRE1* or *bZIP60.*

Next, TuMV-GFP accumulation was examined in systemically infected leaves. The number of plants that became systemically infected were monitored over a time course of 24 dpi (Figure 11A). The percentage of 18 infected plants was recorded at 10 and 17dpi (Figure 11B)

and the average FVs were measured in systemic leaves to monitor the levels of virus accumulation over the 24 day time course (Figure 11C). At 10 dpi 0% of wild-type Col-O plants were systemically infected whereas 22% of *bi-1* and 67% of *bzip60* mutant plants were systemically infected. At 17 dpi, 45% of wilt-type Col-O plants were systemically infected whereas 100% of either *bi-1* or *bzip60* plants were systemically infected at the same time point (Figure 11B). The average FVs in TuMV-GFP systemically infected plants were obtain at 10, 12, 17, 19 and 24 dpi. TuMV-GFP accumulated to higher levels in *bi-1, bzip60* and in *ire1a-2/ire1b-4* mutant plants than in wild-type Col-O plants ($P<0.05$; Figure 11C). These data suggested that TuMV-GFP was equally restricted by *BI-1* or *bZIP60.*

A)

B)

C)

D)
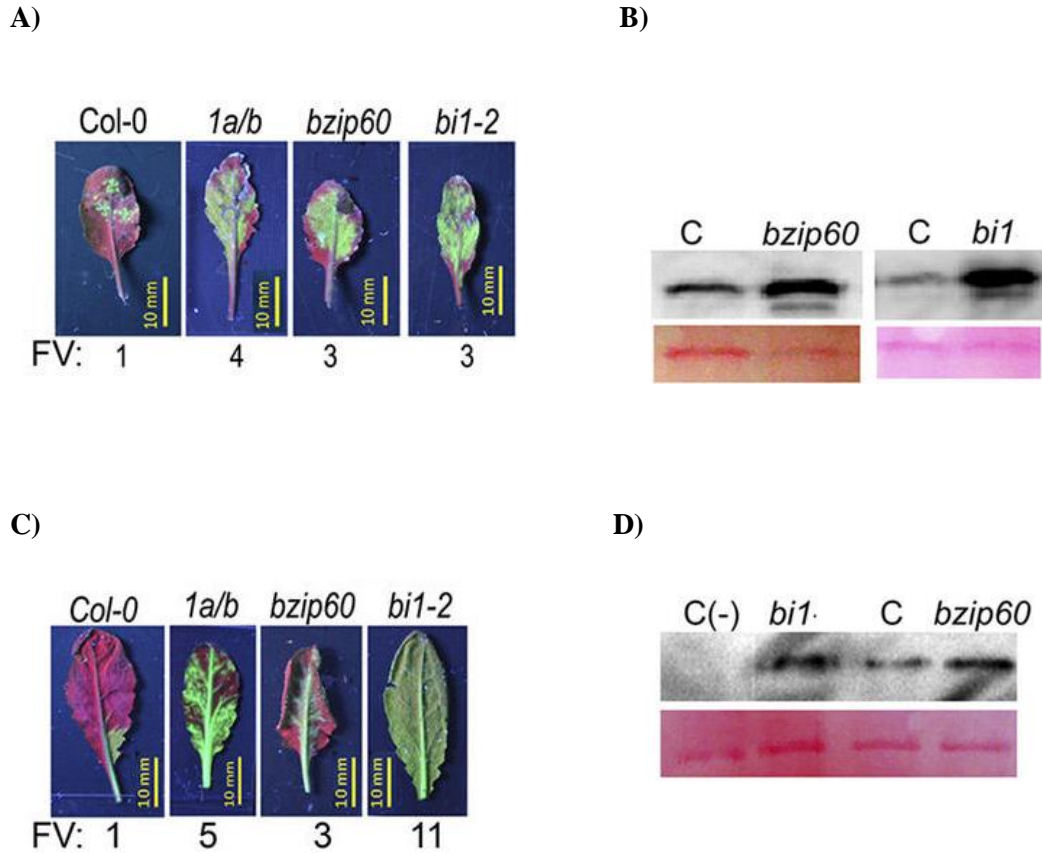
Figure 9: PlAMV-GFP and TuMV-GFP infecting local leaves of *Arabidopsis* plants. For comparisons wild-type Col-O, *bi-1, ire1a-2/ire1b-4* and *bzip60* mutant lines were utilized during the experiments (A) and (C) show representative images of PlAMV-GFP and TuMV-GFP infecting local leaves at 6 days post infiltration (dpi). Average fluorescence values (FVs) from each mutant line with respect to Col-O were written below each photo. All photos were taken with a hand UV lamp. (B) and (D), immunoblots showed the amount of viral coat protein (CP) detected in inoculated leaves with PlAMV-GFP and TuMV-GFP. Lane C represents Col-O and lane C (-) corresponds to healthy controls. Ponceau S staining below immunoblots show equal loading of plant ribosomal protein in each well.

A)

B)

C)

Figure 10: PlAMV-GFP infecting *Arabidopsis* systemic leaves. Wild-type Col-O, *bi-1, ire1a-2/ire1b-4* and *bzip60* mutant lines were utilized during experiments. (A) shows a sequence of representative images of PlAMV-GFP systemic infection in *Arabidopsis* plants from 10 to 24 days post infiltration (dpi). Photos were taken with a UV lamp. Healthy tissues present red color while green tissues represent the virus infected plant tissues. (B), percentage of systemically infected plants at 10 or 12 dpi calculated from 20 plants per wild-type and mutant line. (C), the trend line graph of average fluorescence values (FVs) from six plants per wild-type and mutant line represent the level of PlAMV-GFP accumulation in the systemic tissues of *Arabidopsis* plants at 10, 12, 17, 19 and 24 dpi.

A)

B)

C)

Figure 11: TuMV-GFP infecting *Arabidopsis* systemic leaves. Wild-type Col-O, *bi-1, ire1a-2/ire1b-4* and *bzip60* mutant lines were utilized during experiments. (A) shows a sequence of representative images of TuMV-GFP systemic infection in *Arabidopsis* plants from 10 to 24 days post infiltration (dpi). Photos were taken with a UV lamp. Healthy tissues present red color while green tissues represent the virus infected plant tissues. (B), percentage of systemically infected plants at 10 or 17 dpi calculated from 18 plants per wild type and mutant line. (C), the trend line graph of average fluorescence values (FVs) from six plants per wild-type and mutant line represent the level of TuMV-GFP accumulation in the systemic tissues of *Arabidopsis* plants at 10, 12, 17, 19 and 24 dpi.

Local and systemic PVX-GFP and PVY-GFP infection *bzip60* and *bi-1* silenced *N. benthamiana* plants

Experiments were conducted to determine if silencing *bZIP60* or *BI-1* in *N. benthamiana* leaves leads to greater levels of PVX-GFP or PVY-GFP in inoculated leaves. GFP fluorescence and CP immunoblot analysis were u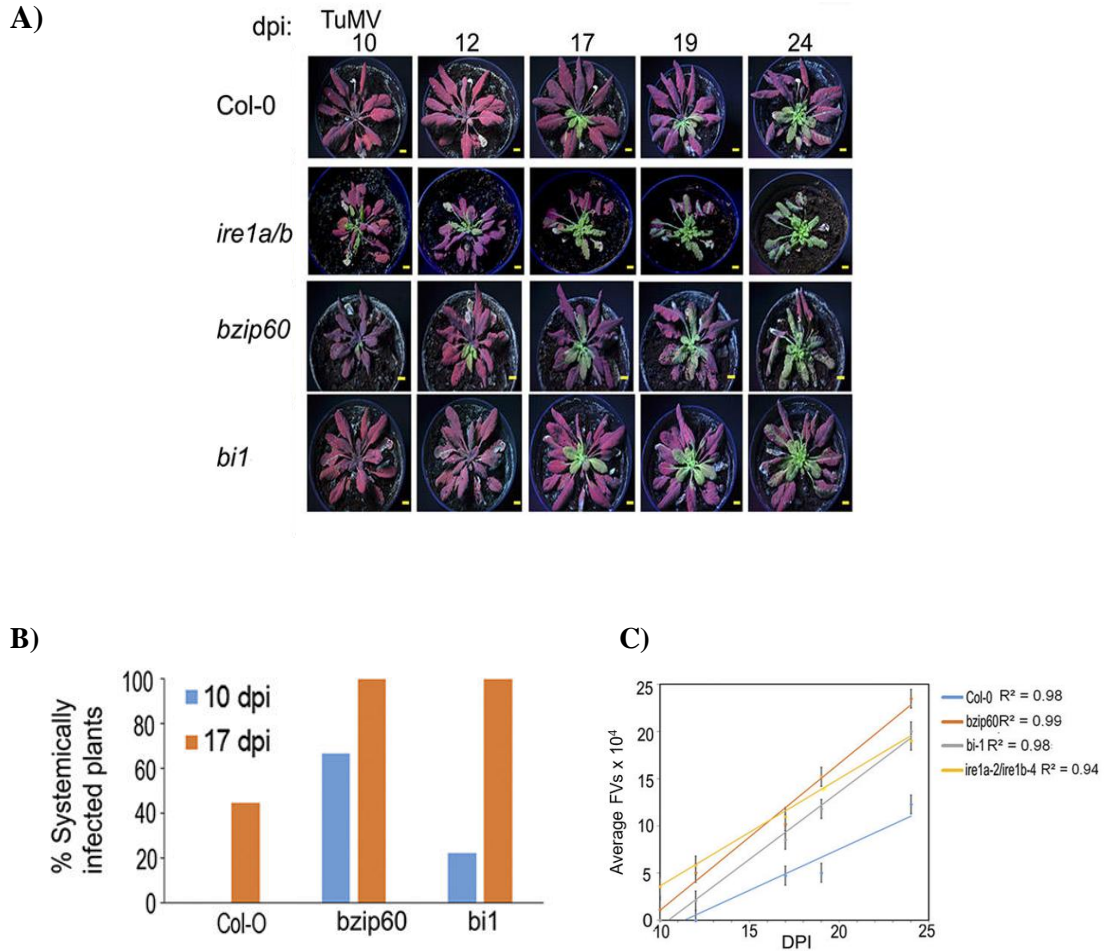sed to monitor virus accumulation in silenced leaves. Dr Dennis Halterman (USDA) prepared pHellsgate-*bzip60si* or pHellsgate-*bi1si* to transiently silence these two genes in *N. benthamiana* plants. Leaves were infiltrated with *Agrobacterium* carrying the pHellsgate-*bzip60si,* pHellsgate-*bi1si* constructs. Semi quantitative RT-PCR assays were conducted to verify that the *bZIP60* and *BI-1* genes were knockdown at 6 days. Samples were amplified for 25, 30, and 35 cycles and then loaded onto 1.5% agarose gels (Figure 12A). The results viewed between 30 and 35 cycles indicated that *bZIP60* or *BI-1* transcripts were reduced 80 to 90% verifying that gene silencing was effective (*P*<0.05; Figure 12A).

PVX-GFP or PVY-GFP with pHellsgate-*bzip60si,* pHellsgate-*bi1si* or *Agrobacterium* (lacking the silencing constructs) were co-delivered to *N. benthamiana* leaves. It was used three samples per treatment and the experiments were repeated three times, and GFP was visualized at 6 dpi. Semi-quantitative RT-PCR was again used to verify knockdown of gene expression in virus inoculated plants. The fluorescence in *bZIP60* or *BI-1* silenced leaves infected with PVX-GFP was greater than in control leaves (Figure 12B). PVY-GFP accumulates slower than PVX-GFP in inoculated leaves and fluorescence was not observed in control or silenced leaves. GFP fluorescence for PVY experiments was not as useful as for PVX-GFP.

Following co-delivery of PVX-GFP or PVY-GFP with the silencing constructs, immunoblot detection was used to determine if the viral CPs were increased in silenced leaves at 6 dpi. Immunoblot analysis revealed higher levels of PVX CP and PVY CP in *bZIP60* or *BI-1* silenced leaves than in control leaves (Figure 12C and D). These data indicated that PVX-GFP and PVY-GFP accumulation increases in the absence of *bZIP60* or *BI-1* in *N. benthamiana*, as for

Arabidopsis plants. These overall data suggested that both *bZIP60* and *BI-1* can restrict PVX-GFP or PVY-GFP infection in inoculated leaves in *N. benthamiana* and *Arabidopsis*.

Systemic PVX-GFP or PVY-GFP infection was monitored to determine if silencing *BI-1* or *bZIP60* leads to increased systemic virus accumulation. GFP from PVX-GFP or PVY-GFP in nine systemic leaves was examined at 14 dpi. GFP fluorescence due to PVX-GFP or PVY-GFP in *BI-1* silenced leaves was higher than in *bZIP60* silenced leaves or control leaves (Figure 13A, B). These data indicated that *BI-1* has a greater role for restricting systemic PVX-GFP or PVY-GFP infection.

Systemic fluorescence was not observed in PVY-GFP infected plants, although the plants were symptomatic. One possibility is that the virus titer was too low to view GFP using a hand-held UV lamp. Therefore qRT-PCR was used to quantify virus genomic RNA accumulation in systemic leaves. At 16 dpi total RNA was extracted and primer sets (Table 1) overlapping the PVY CP ORF were used for qRT-PCR analysis. The levels of PVY genomic RNA in *bZIP60* and *BI-1* silenced leaves were ~3- and 8- fold higher than in control leaves ($P<0.05$; Figure 13C). These data indicated that *BI-1* restricts PVY-GFP to a greater level than *bZIP60*.

Chlorosis and necrosis in *bi-1* and *bzip60* silenced *N. benthamiana* plants treated with PVX-GFP or PVY-GFP

It was observed that silenced plants showed more virus related chlorosis and necrosis than healthy plants. At 6 dpi, PVX-GFP infected and *BI-1* silenced leaves showed severe chlorosis compared to the *bZIP60* silenced or control leaves (Figure 14A). There were no obvious symptoms on PVY-GFP inoculated leaves (Figure 15A).

At 14 dpi, PVX-GFP and PVY-GFP systemically infected *BI-1* silenced plants showed severe stunting, chlorosis and necrosis in the upper crown leaves. PVX-GFP and PVY-GFP systemically infected *bZIP60* silenced plants displayed mosaic symptoms (Figure 14B, C and 15B, C). This information indicated that *BI-1,* a known cell death suppressing protein, protection against virus induced necrosis in *N. benthamiana* plants.

\

A)

B)

C)

D)
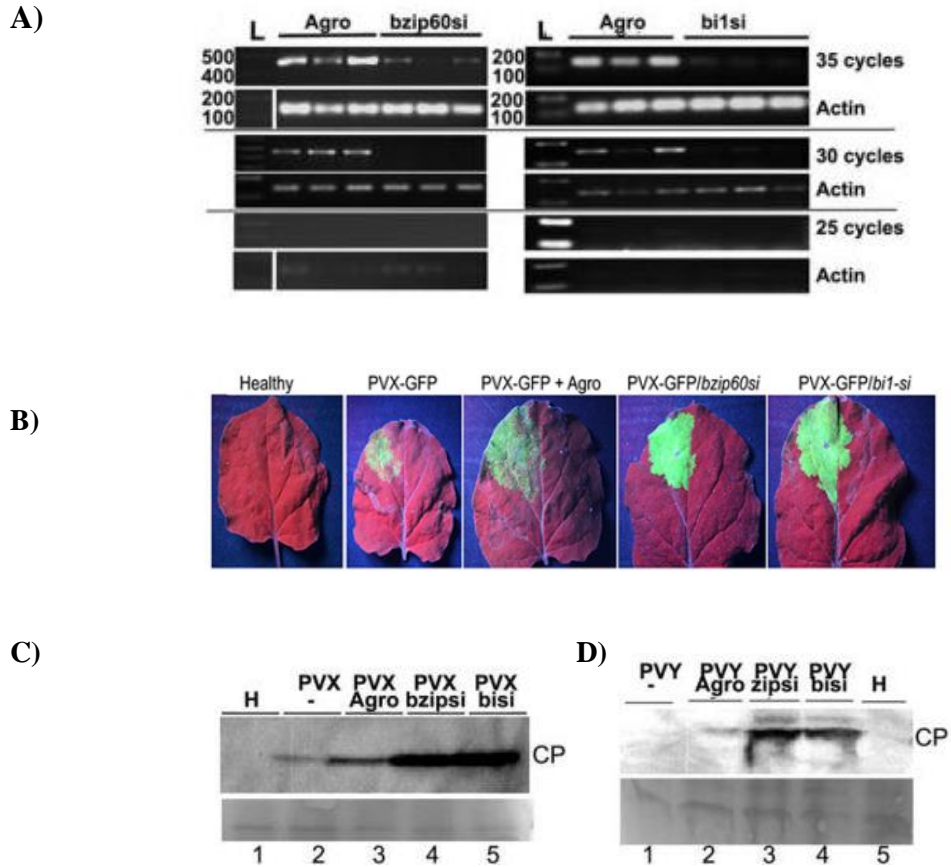
Figure 12: PVY-GFP and PVX-GFP infecting local leaves of *N. benthamiana* plants. (A), semi quantitative qRT-PCR gels for evaluating *bZIP60* and *BI-1* gene silencing efficiency. *Actin II* was utilized as loading control. Amplifications were carried in 35, 30 and 25 cycles. Expected sizes of 100-200 and 400-500 base pairs (bp) are were found for *bZIP60* and *BI-1* genes, respectively. Lanes titled as "Agro" represent samples treated with *Agrobacterium* and no silencing constructs. Lanes named as "*bzip60si*" and "*bi1si*" were *N. benthamiana* leaves agro-infiltrated with pHellsgate-*bzip60si* and pHellsgate-*bi1si* constructs. (B), PVX-GFP infected leaves of *N. benthamiana* at 6 days post infiltration (dpi), photos were taken using UV light. (C) and (D), Immunoblots for detection of PVY-GFP and PVX-GFP viral coat protein (CP) accumulation in detached leaves at 6 dpi (upper image). Ponceau S staining was utilized for assessing equal protein loading in all lanes (lower image). Lanes with the tag H represent healthy control leaves.
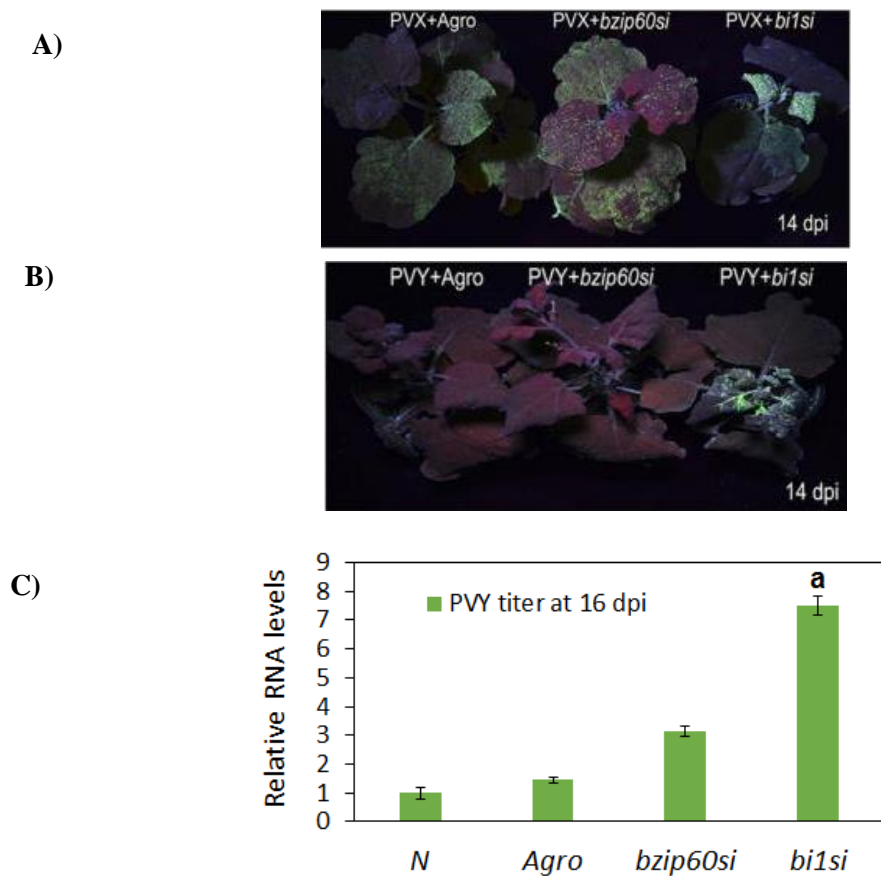
Figure 13: PVY-GFP and PVX-GFP infecting systemic leaves of *N. benthamiana* plants. (A), Images of PVX-GFP infecting *bzip60* and *bi-1* silenced *N. benthamiana* plants, agro delivery without the silencing constructs was also used as control. (B), Images of PVY-GFP infecting *bzip60* and *bi-1* silenced *N. benthamiana* plants, agro-delivery without the silencing constructs was used as control. All images were taken using a UV lamp at 14 days post infiltration (dpi). (C), relative RNA levels of PVY-GFP infecting systemic leaves were measured with qRT-PCR; "*N*" and "*Agro*" represent *N. benthamiana* that were not silenced, "*bzip60si*" and "*bi1si*" columns represent systemic leaves treated with pHellsgate-*bzip60si* and pHellsgate-*bi1si* constructs. RNA from systemic leaves was extracted at 16 dpi. Error bars represent the level of standard deviation in each treatment. ANOVA and Tukey methods were used for evaluating statistical differences. Bars that were statically different were identified with the letter "a" for a significance level of ($P<0.05$).

A)

B)

C)
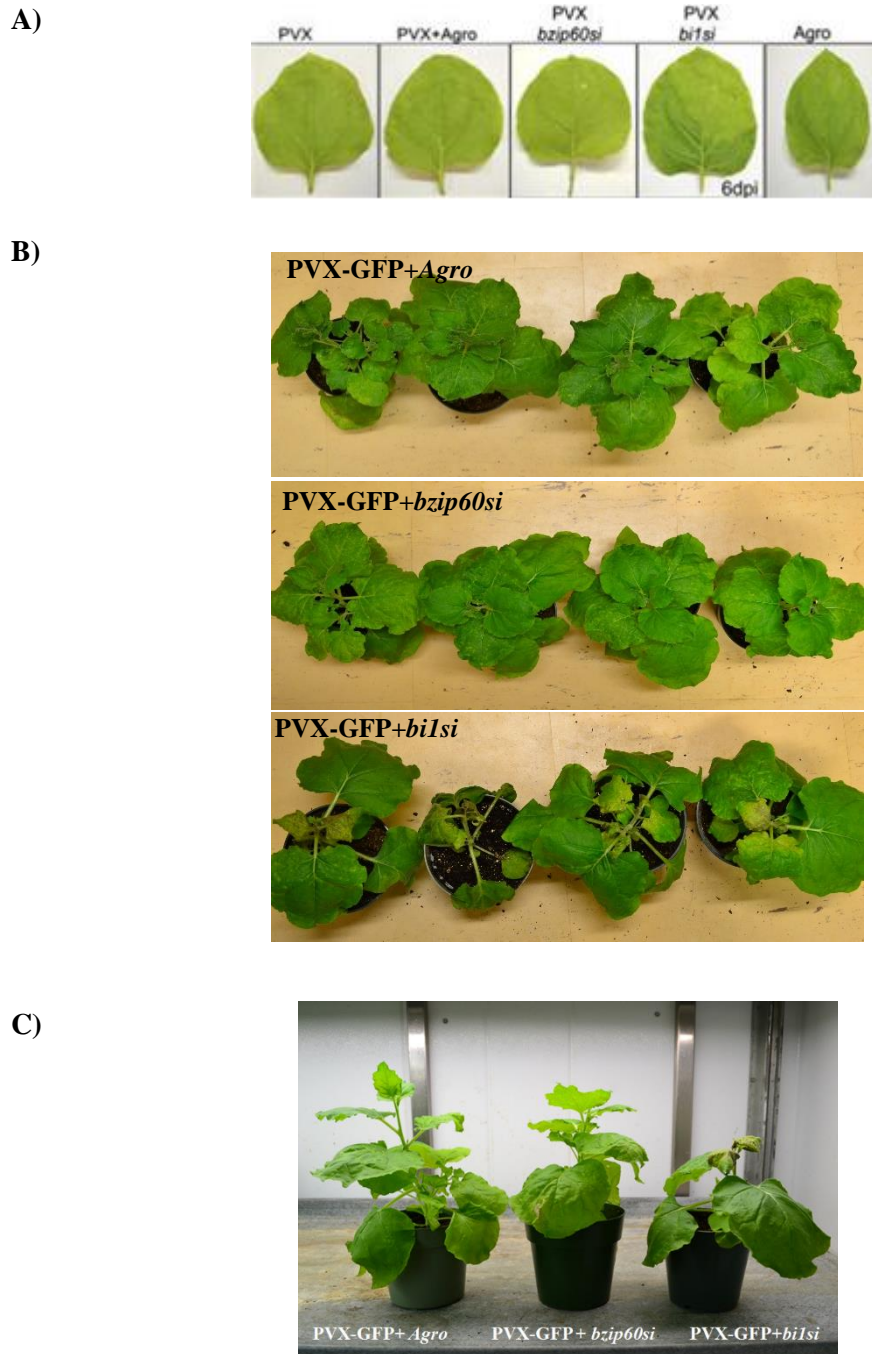
Figure 14: photos of PVX-GFP infecting *N. benthamiana* plants. (A) necrosis in inoculated leaves that had co delivery of PVX-GFP with pHellsgate-*bzip60si,* pHellsgate-*bi1si* or *Agrobacterium* lacking the silencing constructs at 6 days post infiltration (dpi). (B) and (C) necrotic symptoms in systemic leaves at 14 dpi.

A)
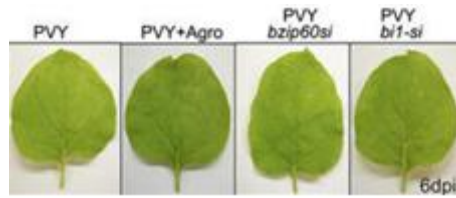
B)
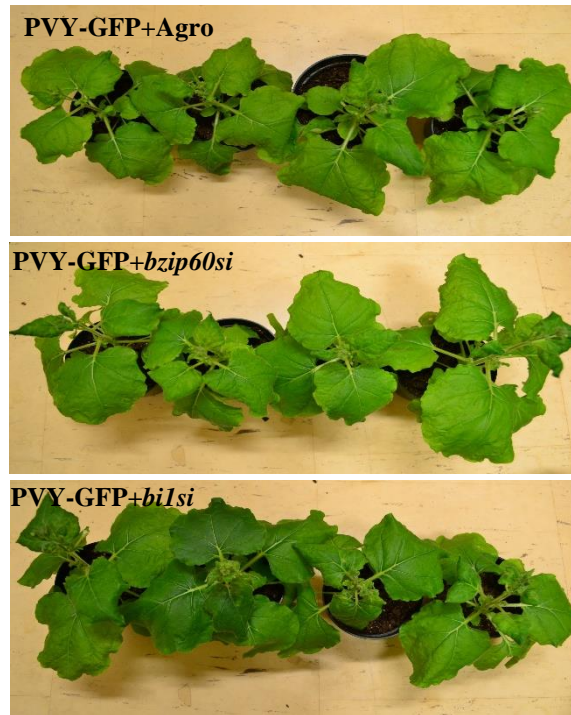
C)

Figure 15: photos of PVY-GFP infecting *N. benthamiana* plants. (A) necrosis in inoculated leaves that had co delivery of PVY-GFP with pHellsgate-*bzip60si,* pHellsgate-*bi1si* or *Agrobacterium* lacking the silencing constructs at 6 days post infiltration (dpi). (B) and (C) necrotic symptoms in systemic leaves at 14 dpi.

CHAPTER V

DISCUSSION AND CONCLUSSIONS

PlAMV-GFP or TuMV-GFP infection levels were different depending upon the *IRE1* gene. PlAMV-GFP accumulation in inoculated and systemic leaves is higher in plants defective in *IRE1a* than in wild type or *IRE1b* defective plants. TuMV-GFP accumulation is equally dependent upon the active presence of *IRE1a* and *IRE1b* in inoculated leaves, and systemic accumulation seems to be greatly affected by mutations in *IRE1b* than in *IRE1a*. Mutations in both *IRE1a* and *IRE1b* lead to higher local PlAMV-GFP and TuMV-GFP accumulation levels which suggest that one gene can provide support when the other gene is deleted. The IRE1 protein has two enzymatic domains, an RNAse domain for splicing bZIP60 mRNA or for RIDD mRNA targets, and a kinase domain for auto-phosphorylation (Deng *et al.*, 2013b; Korner *et al.*, 2015). IRE1a and IRE1b proteins have different kinase loops which may mean they do not have the same phosphorylation targets (Moreno *et al.*, 2012). Researchers reported that IRE1b plays a greater role in *bZIP60* mRNA splicing than IRE1a during ER stress (Deng *et al.*, 2011; Humbert *et al.*, 2012). This suggested that the two *IRE1* genes may act preferentially on certain functions. There are factors identified in eukaryotes that bind IRE1 proteins, but this list is incomplete.

It is known that CPR5 in plants interacts with IRE1 and is activated by salicylic acid during defense (Meng *et al.*, 2017).   In mammals, BiP binds IRE1, but it is not known if that interaction occurs in plants (Chen *et al.*, 2013). BiP is also associated with co-chaperone AtERDj3A and it is reasonable to consider that the cochaperone may be involved in IRE1 interactions along with BiP (Chen *et al.*, 2012).

The PlAMV TGB3 preferentially interacts with IRE1a recognition strategies whereas TuMV 6K2 seems to engage both IRE1 proteins in the inoculated leaves. These data suggested that these viral proteins may engage different domains of IRE1 or intermediary factors leading to activation of UPR and *bZIP60* mRNA splicing. *IRE1a* and *IRE1b* have been observed to provide some unique and some overlapping activities in response to ER stress in *Arabidopsis* after exposure with ER stress chemical inducer tunicamycin (Chen *et al.*, 2012; Wan *et al.*, 2016). Although it was not discovered whether either *IRE1* gene restrict viral replication, further experiments should be conducted to establish potential roles of *IRE1* in virus multiplication.

ER localized transcription factors *bZIP17*, *bZIP28* and *bZIP60* are key components of UPR responses during ER stress signaling (Deng *et al.*, 2013a). Their transcript accumulation levels were evaluated following agro-delivery of the potexvirus TGB3 or potyvirus 6K2 in *Arabidopsis* and *N. benthamiana*. Prior studies demonstrated that *bZIP60* mRNA is induced by the PVX TGB3 and TuMV 6K2 (Ye *et al.*, 2011; Ye *et al.*, 2013; Zhang *et al.*, 2015). The data presented in this thesis confirms *bZIP60* mRNA is induced by more than one potexvirus TGB3 or potyvirus 6K2 in two different host species. These data also indicated that gene activation is a conserved function of these viral proteins.

Prior reports indicated that *bZIP17* and *bZIP28* are primarily induced by abiotic stressors (Liu *et al.*, 2007b, 2007a; Liu *et al.*, 2010). This is the first evidence that *bZIP17* and *bZIP28* transcripts are elevated following agro-delivery of potexvirus TGB3 or potyvirus 6K2. Although

bZIP17 is not induced by PVX TGB3 in either host, it is elevated in *Arabidopsis* (but not *N. benthamiana*) following delivery of TuMV 6K2. *bZIP17* and *bZIP28* typically are activated by abiotic factors such as ABA, heat, or salt (Liu *et al.*, 2007b, 2007a; Zhou *et al.*, 2015). bZIP60 is more often associated with SA and plant innate immunity as well certain other abiotic stressors. One study showed that treatment of *Arabidopsis* leaves with the polyamine, spermine led to transcriptional upregulation of *bZIP60*, *bZIP28* and *bZIP17* (Sagor *et al.*, 2015). This study demonstrated that spermine is a general activator of these three UPR related pathways. Spermine synthase is activated in *RCY1* resistance gene to *Cucumber mosaic virus* (CMV) strain Y (Mitsuya *et al.*, 2009; Sagor *et al.*, 2015). Increase in spermine in the cell can cause calcium release from the ER lumen which leads to UPR (Pottosin *et al.*, 2014). In this study it is proposed that the potexvirus TGB3 and potyvirus 6K2 proteins, which insert into the ER membrane, may cause some changes in ER calcium stores and this could indirectly lead to general activation of *bZIP28* and *bZIP17* related pathways. However, there is not direct evidence that bZIP60, bZIP28, or bZIP17 move from the ER to the nucleus.

Virus accumulation in *Arabidopsis* plants that were defective for *bZIP17*, *bZIP28* or *bZIP60* were analyzed and compared. It was found that PlAMV-GFP accumulation was higher in plants defective for *bZIP60* and/or *bZIP17* than wild-type or *bzip28*-mutant plants. TuMV-GFP accumulation was higher in plants defective for *bZIP60* and/or *bZIP28* than in wild-type or *bzip17* mutant plants. These data suggested that *bZIP60* is a factor in host susceptibility to both viruses whereas *bZIP28* and *bZIP17* differentially restrict potyvirus and potexvirus infection. The ability of *bZIP17* and *bZIP28* to respond differently to certain stressors has been documented (Ruberti *et al.*, 2015; Wan *et al.*, 2016). It is known that *bZIP28* reacts mainly to heat and cold stress while *bZIP17* is mostly involved in salt stress (Liu *et al.*, 2007b, 2007a; Deng *et al.*, 2011; Wan *et al.*, 2016). Further experiments are needed to determine if these factors differently engage the TGB3 and 6K2 proteins.

Prior research conducted in yeast two hybrid systems have demonstrated that *bZIP17, bZIP28* and *bZIP60* form heterodimers (Liu *et al.*, 2010). These heterodimers exist within a transcription activation complex sitting down on a promoter to activate certain ER stress responsive genes (Llorca *et al.*, 2014). Based on this model, it was suggested a scenario in which bZIP60 and bZIP17 associate to activate genes that restrict PlAMV movement. Alternatively bZIP60 and bZIP28 could associate to activate genes that restrict TuMV movement.

Arabidopsis and *S. tuberosum* have three *BiP* candidate genes and *N. benthamiana* has six *BiP*, these are differentially activated by *bZIP17*, *bZIP28* and *bZIP60*. It was conducted qRT-PCR experiments to measure the transcript level of *BiP* candidates in *Arabidopsis*, *N. benthamiana* and *S. tuberosum* in response to agro-delivery of PlAMV TGB3, PVX TGB3, TuMV 6K2 or PVY 6K2 genes. In *Arabidopsis,* agro-delivery of each TGB3 and 6K2 led to higher levels of *AtBiP3,* but *AtBiP1* and *AtBiP2* transcript accumulation was elevated following agro-delivery of TuMV 6K2 or PVY 6K2. IRE1 splices *bZIP60* mRNA and the transcription factor bZIP60s moves to the nucleus and upregulates *BiP3* transcription (Liu *et al.*, 2010). bZIP17 and bZIP28 also regulate transcription of *BiP1, 2*, and *3* (Iwata *et al.*, 2008; Henriquez-Valencia *et al.*, 2015). BiP1 and BiP3 proteins bind bZIP28 and bZIP17 in the ER and suppress their release from the ER membrane (Srivastava *et al.*, 2013). This becomes an autoregulatory process whereby the bZIP transcription factors activate BiP expression to increase protein folding in the ER lumen, but also to shut down their own activation in the ER and restore the cell to homeostasis. BIP2 binds another factor known as AtBAG7, which is a cell death regulating protein located in the ER (Williams. *et al.*, 2010). AtBAG7 can form a heterodimer with bZIP28 (Li *et al.*, 2016c). This is interesting because it appears that the potyvirus 6K2 proteins may play a role in activating *BiP2* which potentially could lead to downregulation of the cell death regulator *AtBAG7*.

In *N. benthamiana*, the transcript levels of *NbBiP1*, *NbBiP2, NbBiP3, NbBiP5* and *NbBiP8* orthologues and in *S. tuberosum*, *StBiP-D3* and *StBiP-D5* but not *StBiP-A* were induced upon treatment with PVX TGB3 or PVY 6K2. Activation of *BiP* mediated by viral genes resembles prior studies in which treatments with treatments with PVX TGB3 demonstrated a significant *BiP* induction (Ye *et al.*, 2011; Ye *et al.*, 2013). Therefore, this study sheds light on the identification of new *BiP* candidates that can activate in response to virus assault.

This study wanted to determine if cell death suppressor *BI-1*, and UPR genes *IRE1* and *bZIP60* similarly impact the ability of PlAMV-GFP or TuMV-GFP to spread locally and systemically in *Arabidopsis* plants. Prior reports proposed a model in which BI-1 binds to IRE1 and downregulates *bZIP60* mRNA splicing (Lisbona *et al.*, 2009; Ishikawa *et al.*, 2011b). Based on this model it would expect that knockout of *BI-1, IRE1* or *bZIP60* should similarly alter the patterns of virus accumulation in local and systemic leaves. Moreover, in this study it was hypothesized that *BI-1* expression was controlled by *IRE1* and *bZIP60*. The data indicated that PlAMV accumulation in local leaves is comparably higher in *bi-1, ire1a-2/ire1b-4*, and *bzip60* mutant plants however TuMV infection was 11 fold higher than in wild-type leaves and 2-3 fold higher than in *ire1a-2/ire1b-4* and *bzip60* mutant plants. One hundred percent of *bi-1* inoculated plants were systemically infected at 10 and 17 dpi with PlAMV-GFP and TuMV-GFP. These data suggested that *bi-1* has a more significant effect on systemic accumulation than *bZIP60*. Similarly, the experiments conducted in *bi1si-* and *bzip60si- N. benthamiana* plants infected with PVX-GFP or PVY-GFP revealed *BI-1* greater role for restricting virus movement than *bZIP60*.

Prior work has shown that *BI-1* is linked to plant defense responses and functions in the ER (Eichmann *et al.*, 2012). In two studies *BI-1* knockdowns led to enhanced susceptibility to *P. syringae* and *B. graminis (*Kawai-Yamada *et al., 2009;* Weis *et al., 2013)*. bZIP60 is also engaged in regulating susceptibility to *P. syringae* (Moreno *et al.*, 2012)*. The *E. coli* bacterial effector NIeH can target *BI-1* to inhibit cell death responses (Robinson *et al.*, 2016). Evidence that

bacterial effectors control activation of BI-1 and other ER stress responses, suggests that the ability of the TGB3 and 6K2 to act on these pathways, may suggest that these viral proteins are also effectors. Pathogen effectors are proteins that interact with a host protein involved in defense recognition (Gouveia *et al.*, 2016). The data provided in this thesis showed that knockdown of the ER stress sensors led to greater virus accumulation. While there was lack of evidence of direct interactions between the viral proteins and these ER stress sensors, it is reasonable to suggest that the UPR pathways provide some protection against virus infection and that the TGB3 and 6K2 proteins may act as effectors of these viral suppressive pathways.

REFERENCES

Aparicio, F., Thomas, C. L., Lederer, C., Niu, Y., Wang, D., & Maule, A. J. (2005). Virus induction of heat shock protein 70 reflects a general response to protein accumulation in the plant cytosol. *Plant Physiol, 138*(1), 529-536. doi: 10.1104/pp.104.058958

Arias Gaguancela, O. P., Zuniga, L. P., Arias, A. V., Halterman, D., Flores, F. J., Johansen, I. E., Wang, A., Yamaji, Y., & Verchot-Lubicz, J. (2016). The IRE1/bZIP60 pathway and Bax inhibitor 1 suppress systemic accumulation of potyviruses and potexviruses in *Arabidopsis* and *N. benthamiana* plants. *Mol Plant Microbe Interact*. doi: 10.1094/mpmi-07-16-0147-r

Bamunusinghe, D., Hemenway, C. L., Nelson, R. S., Sanderfoot, A. A., Ye, C. M., Silva, M. A., Payton, M., & Verchot-Lubicz, J. (2009). Analysis of *potato virus X* replicase and TGBp3 subcellular locations. *Virology, 393*(2), 272-285. doi: 10.1016/j.virol.2009.08.002

Bradford, M. M. (1976). A rapid and sensitive method for the quantitation of microgram quantities of protein utilizing the principle of protein-dye binding. *Anal Biochem, 72*, 248-254.

Carolino, S. M. B., Vaez, J. R., Irsigler, A. S. T., Valente, M. A. S., Rodrigues, L. A. Z., & Fontes, E. P. B. (2003). Plant *BiP* gene family: differential expression, stress induction and protective role against physiological stresses. *Brazilian Journal of Plant Physiology, 15*, 59-66.

Carvalho, H. H., Silva, P. A., Mendes, G. C., Brustolini, O. J., Pimenta, M. R., Gouveia, B. C., Valente, M. A., Ramos, H. J., Soares-Ramos, J. R., & Fontes, E. P. (2014). The endoplasmic reticulum binding protein BiP displays dual function in modulating cell death events. *Plant Physiol, 164*(2), 654-670. doi: 10.1104/pp.113.231928

Chen, Y., & Brandizzi, F. (2012). AtIRE1A/AtIRE1B and AGB1 independently control two essential unfolded protein response pathways in *Arabidopsis*. *Plant J, 69*(2), 266-277. doi: 10.1111/j.1365-313X.2011.04788.x

Chen, Y., & Brandizzi, F. (2013). IRE1: ER stress sensor and cell fate executor. *Trends Cell Biol, 23*(11), 547-555. doi: 10.1016/j.tcb.2013.06.005

Cheng, N. H., Su, C. L., Carter, S. A., & Nelson, R. S. (2000). Vascular invasion routes and systemic accumulation patterns of *Tobacco mosaic virus* in *Nicotiana benthamiana*. *Plant J, 23*(3), 349-362.

Chou, Y. L., Hung, Y. J., Tseng, Y. H., Hsu, H. T., Yang, J. Y., Wung, C. H., Lin, N. S., Meng, M., Hsu, Y. H., & Chang, B. Y. (2013). The stable association of virion with the triple-gene-block protein 3-based complex of *Bamboo mosaic virus*. *PLoS Pathog, 9*(6), e1003405. doi: 10.1371/journal.ppat.1003405

Chung, B. Y., Miller, W. A., Atkins, J. F., & Firth, A. E. (2008). An overlapping essential gene in the Potyviridae. *Proc Natl Acad Sci U S A, 105*(15), 5897-5902. doi: 10.1073/pnas.0800468105

Cotton, S., Grangeon, R., Thivierge, K., Mathieu, I., Ide, C., Wei, T., Wang, A., & Laliberté, J.-F. (2009). *Turnip Mosaic Virus* RNA Replication Complex Vesicles Are Mobile, Align with Microfilaments, and Are Each Derived from a Single Viral Genome. *Journal of Virology, 83*(20), 10460-10471. doi: 10.1128/JVI.00819-09

Cui, H., & Wang, A. (2016). Plum Pox Virus 6K1 Protein Is Required for Viral Replication and Targets the Viral Replication Complex at the Early Stage of Infection. *J Virol, 90*(10), 5119-5131. doi: 10.1128/jvi.00024-16

Cui, X., Wei, T., Chowda-Reddy, R. V., Sun, G., & Wang, A. (2010). The *Tobacco etch virus* P3 protein forms mobile inclusions via the early secretory pathway and traffics along actin microfilaments. *Virology, 397*(1), 56-63. doi: 10.1016/j.virol.2009.11.015

Curtis, M. D., & Grossniklaus, U. (2003). A Gateway Cloning Vector Set for High-Throughput Functional Analysis of Genes in Planta. *Plant Physiol, 133*(2), 462-469. doi: 10.1104/pp.103.027979

Deng, Y., Humbert, S., Liu, J. X., Srivastava, R., Rothstein, S. J., & Howell, S. H. (2011). Heat induces the splicing by IRE1 of a mRNA encoding a transcription factor involved in the unfolded protein response in *Arabidopsis*. *Proc Natl Acad Sci U S A, 108*(17), 7247-7252. doi: 10.1073/pnas.1102117108

Deng, Y., Srivastava, R., & Howell, S. H. (2013a). Endoplasmic reticulum (ER) stress response and its physiological roles in plants. *Int J Mol Sci, 14*(4), 8188-8212. doi: 10.3390/ijms14048188

Deng, Y., Srivastava, R., & Howell, S. H. (2013b). Protein kinase and ribonuclease domains of IRE1 confer stress tolerance, vegetative growth, and reproductive development in *Arabidopsis*. *Proc Natl Acad Sci U S A, 110*(48), 19633-19638. doi: 10.1073/pnas.1314749110

Duwi Fanata, W. I., Lee, S. Y., & Lee, K. O. (2013). The unfolded protein response in plants: a fundamental adaptive cellular response to internal and external stresses. *J Proteomics, 93*, 356-368. doi: 10.1016/j.jprot.2013.04.023

Eichmann, R., & Schäfer, P. (2012). The endoplasmic reticulum in plant immunity and cell death. *Front Plant Sci, 3*, 200. doi: 10.3389/fpls.2012.00200

Gouveia, B. C., Calil, I. P., Machado, J. P., Santos, A. A., & Fontes, E. P. (2016). Immune Receptors and Co-receptors in Antiviral Innate Immunity in Plants. *Front Microbiol, 7*, 2139. doi: 10.3389/fmicb.2016.02139

Grangeon, R., Jiang, J., Wan, J., Agbeci, M., Zheng, H., & Laliberte, J. F. (2013). 6K2-induced vesicles can move cell to cell during *Turnip mosaic virus* infection. *Front Microbiol, 4*, 351. doi: 10.3389/fmicb.2013.00351

Harries, P., & Ding, B. (2011). Cellular factors in plant virus movement: At the leading edge of macromolecular trafficking in plants. *Virology*(411), 237-243.

Heinlein, M. (2015). Plant virus replication and movement. *Virology, 479–480*, 657-671. doi: http://dx.doi.org/10.1016/j.virol.2015.01.025

Henriquez-Valencia, C., Moreno, A. A., Sandoval-Ibanez, O., Mitina, I., Blanco-Herrera, F., Cifuentes-Esquivel, N., & Orellana, A. (2015). bZIP17 and bZIP60 Regulate the Expression of BiP3 and Other Salt Stress Responsive Genes in an UPR-Independent Manner in *Arabidopsis thaliana*. *J Cell Biochem, 116*(8), 1638-1645. doi: 10.1002/jcb.25121

Hipper, C., Brault, V., Ziegler-Graff, V., & Revers, F. (2013). Viral and cellular factors involved in Phloem transport of plant viruses. *Front Plant Sci, 4*, 154. doi: 10.3389/fpls.2013.00154

Hollien, J. (2013). Evolution of the unfolded protein response. *Biochim Biophys Acta, 1833*(11), 2458-2463. doi: 10.1016/j.bbamcr.2013.01.016

Hong, X.-Y., Chen, J., Shi, Y.-H., & Chen, J.-P. (2007). The '6K1' protein of a strain of *Soybean mosaic virus* localizes to the cell periphery. *Arch Virol, 152*(8), 1547-1551. doi: 10.1007/s00705-007-0972-7

Hu, X., Nie, X., He, C., & Xiong, X. (2011). Differential pathogenicity of two different recombinant PVY(NTN) isolates in Physalis floridana is likely determined by the coat protein gene. *Virol J, 8*, 207. doi: 10.1186/1743-422x-8-207

Huang, Y. L., Han, Y. T., Chang, Y. T., Hsu, Y. H., & Meng, M. (2004). Critical residues for GTP methylation and formation of the covalent m7GMP-enzyme intermediate in the capping enzyme domain of *Bamboo mosaic virus*. *J Virol, 78*(3), 1271-1280.

Humbert, S., Zhong, S., Deng, Y., Howell, S. H., & Rothstein, S. J. (2012). Alteration of the bZIP60/IRE1 Pathway Affects Plant Response to ER Stress in *Arabidopsis thaliana*. *PLoS One, 7*(6), e39023. doi: 10.1371/journal.pone.0039023

Ishikawa, T., Watanabe, N., Nagano, M., Kawai-Yamada, M., & Lam, E. (2011a). Bax inhibitor-1: a highly conserved endoplasmic reticulum-resident cell death suppressor. *Cell Death Differ, 18*(8), 1271-1278. doi: 10.1038/cdd.2011.59

Ishikawa, T., Watanabe, N., Nagano, M., Kawai-Yamada, M., & Lam, E. (2011b). Bax inhibitor-1: a highly conserved endoplasmic reticulum-resident cell death suppressor. *Cell Death Differ, 18*(8), 1271-1278. doi: 10.1038/cdd.2011.59

Ivanov, K. I., Eskelin, K., Lohmus, A., & Makinen, K. (2014). Molecular and cellular mechanisms underlying potyvirus infection. *J Gen Virol, 95*(Pt 7), 1415-1429. doi: 10.1099/vir.0.064220-0

Ivanov, K. I., & Makinen, K. (2012). Coat proteins, host factors and plant viral replication. *Curr Opin Virol, 2*(6), 712-718. doi: 10.1016/j.coviro.2012.10.001

Iwata, Y., Fedoroff, N. V., & Koizumi, N. (2008). *Arabidopsis* bZIP60 Is a Proteolysis-Activated Transcription Factor Involved in the Endoplasmic Reticulum Stress Response. *Plant Cell, 20*(11), 3107-3121. doi: 10.1105/tpc.108.061002

Jiang, J., Patarroyo, C., Garcia Cabanillas, D., Zheng, H., & Laliberte, J. F. (2015). The Vesicle-Forming 6K2 Protein of *Turnip Mosaic Virus* Interacts with the COPII Coatomer Sec24a for Viral Systemic Infection. *J Virol, 89*(13), 6695-6710. doi: 10.1128/jvi.00503-15

Johnson, J. A., Bragg, J. N., Lawrence, D. M., & Jackson, A. O. (2003). Sequence elements controlling expression of *Barley stripe mosaic virus* subgenomic RNAs in vivo. *Virology, 313*(1), 66-80.

Ju, H. J., Brown, J. E., Ye, C. M., & Verchot-Lubicz, J. (2007). Mutations in the central domain of *Potato virus X* TGBp2 eliminate granular vesicles and virus cell-to-cell trafficking. *J Virol, 81*(4), 1899-1911. doi: 10.1128/jvi.02009-06

Kawai-Yamada, M., Hori, Z., Ogawa, T., Ihara-Ohori, Y., Tamura, K., Nagano, M., Ishikawa, T., & Uchimiya, H. (2009). Loss of calmodulin binding to Bax inhibitor-1 affects Pseudomonas-mediated hypersensitive response-associated cell death in *Arabidopsis* thaliana. *J Biol Chem, 284*(41), 27998-28003. doi: 10.1074/jbc.M109.037234

Komatsu, K., Hashimoto, M., Maejima, K., Shiraishi, T., Neriya, Y., Miura, C., Minato, N., Okano, Y., Sugawara, K., Yamaji, Y., & Namba, S. (2011). A necrosis-inducing elicitor domain encoded by both symptomatic and asymptomatic *Plantago asiatica mosaic virus* isolates, whose expression is modulated by virus replication. *Mol Plant Microbe Interact, 24*(4), 408-420. doi: 10.1094/mpmi-12-10-0279

Komatsu, K., Yamaji, Y., Ozeki, J., Hashimoto, M., Kagiwada, S., Takahashi, S., & Namba, S. (2008). Nucleotide sequence analysis of seven Japanese isolates of *Plantago asiatica mosaic virus* (PlAMV): a unique potexvirus with significantly high genomic and biological variability within the species. *Arch Virol, 153*(1), 193-198. doi: 10.1007/s00705-007-1078-y

Korner, C. J., Du, X., Vollmer, M. E., & Pajerowska-Mukhtar, K. M. (2015). Endoplasmic Reticulum Stress Signaling in Plant Immunity--At the Crossroad of Life and Death. *Int J Mol Sci, 16*(11), 26582-26598. doi: 10.3390/ijms161125964

Li, Y., & Dickman, M. (2016a). Processing of AtBAG6 triggers autophagy and fungal resistance. *Plant Signal Behav, 11*(6), e1175699. doi: 10.1080/15592324.2016.1175699

Li, Y., Kabbage, M., Liu, W., & Dickman, M. B. (2016b). Aspartyl Protease-Mediated Cleavage of BAG6 Is Necessary for Autophagy and Fungal Resistance in Plants. *Plant Cell, 28*(1), 233-247. doi: 10.1105/tpc.15.00626

Li, Y., Williams, B., & Dickman, M. (2016c). *Arabidopsis* B-cell lymphoma2 (Bcl-2)-associated athanogene 7 (BAG7)-mediated heat tolerance requires translocation, sumoylation and binding to WRKY29. *New Phytol*. doi: 10.1111/nph.14388

Lisbona, F., Rojas-Rivera, D., Thielen, P., Zamorano, S., Todd, D., Martinon, F., Glavic, A., Kress, C., Lin, J. H., Walter, P., Reed, J. C., Glimcher, L. H., & Hetz, C. (2009). BAX inhibitor-1 is a negative regulator of the ER stress sensor IRE1alpha. *Mol Cell, 33*(6), 679-691. doi: 10.1016/j.molcel.2009.02.017

Liu, J. X., & Howell, S. H. (2010). bZIP28 and NF-Y transcription factors are activated by ER stress and assemble into a transcriptional complex to regulate stress response genes in *Arabidopsis*. *Plant Cell, 22*(3), 782-796. doi: 10.1105/tpc.109.072173

Liu, J. X., Srivastava, R., Che, P., & Howell, S. H. (2007a). An endoplasmic reticulum stress response in *Arabidopsis* is mediated by proteolytic processing and nuclear relocation of a membrane-associated transcription factor, bZIP28. *Plant Cell, 19*(12), 4111-4119. doi: 10.1105/tpc.106.050021

Liu, J. X., Srivastava, R., Che, P., & Howell, S. H. (2007b). Salt stress responses in *Arabidopsis* utilize a signal transduction pathway related to endoplasmic reticulum stress signaling. *Plant J, 51*(5), 897-909. doi: 10.1111/j.1365-313X.2007.03195.x

Llorca, C. M., Potschin, M., & Zentgraf, U. (2014). bZIPs and WRKYs: two large transcription factor families executing two different functional strategies. *Front Plant Sci, 5*, 169. doi: 10.3389/fpls.2014.00169

Meng, Z., Ruberti, C., Gong, Z., & Brandizzi, F. (2017). CPR5 modulates salicylic acid and the unfolded protein response to manage tradeoffs between plant growth and stress responses. *The Plant Journal, 89*(3), 486-501. doi: 10.1111/tpj.13397

Mitsuya, Y., Takahashi, Y., Berberich, T., Miyazaki, A., Matsumura, H., Takahashi, H., Terauchi, R., & Kusano, T. (2009). Spermine signaling plays a significant role in the defense response of *Arabidopsis thaliana* to cucumber mosaic virus. *J Plant Physiol, 166*(6), 626-643. doi: 10.1016/j.jplph.2008.08.006

Mlotshwa, S., Pruss, G. J., MacArthur, J. L., & Reed, J. W. (2016). Developmental Defects Mediated by the P1/HC-Pro Potyviral Silencing Suppressor Are Not Due to Misregulation of AUXIN RESPONSE FACTOR 8. *172*(3), 1853-1861.

Moreno, A. A., Mukhtar, M. S., Blanco, F., Boatwright, J. L., Moreno, I., Jordan, M. R., Chen, Y., Brandizzi, F., Dong, X., Orellana, A., & Pajerowska-Mukhtar, K. M. (2012). IRE1/bZIP60-mediated unfolded protein response plays distinct roles in plant immunity and abiotic stress responses. *PLoS One, 7*(2), e31944. doi: 10.1371/journal.pone.0031944

Ni, D., Xu, P., & Gallagher, S. (2016). Immunoblotting and Immunodetection. *Curr Protoc Immunol, 114*, 8.10.11-18.10.36. doi: 10.1002/cpim.10

Niehl, A., Amari, K., Gereige, D., Brandner, K., Mely, Y., & Heinlein, M. (2012). Control of *Tobacco mosaic virus* movement protein fate by CELL-DIVISION-CYCLE protein48. *Plant Physiol, 160*(4), 2093-2108. doi: 10.1104/pp.112.207399

Nummert, G., Somera, M., Uffert, G., Abner, E., & Truve, E. (2017). P1-independent replication and local movement of *Rice yellow mottle virus* in host and non-host plant species. *Virology, 502*, 28-32. doi: 10.1016/j.virol.2016.12.007

Park, M.-R., Jeong, R.-D., & Kim, K.-H. (2014). Understanding the intracellular trafficking and intercellular transport of potexviruses in their host plants. *Front Plant Sci, 5*, 60. doi: 10.3389/fpls.2014.00060

Park, M. R., Seo, J. K., & Kim, K. H. (2013). Viral and nonviral elements in potexvirus replication and movement and in antiviral responses. *Adv Virus Res, 87*, 75-112. doi: 10.1016/b978-0-12-407698-3.00003-x

Pfaffl, M. W., Horgan, G. W., & Dempfle, L. (2002). Relative expression software tool (REST) for group-wise comparison and statistical analysis of relative expression results in real-time PCR. *Nucleic Acids Res, 30*(9), e36.

Pottosin, I., & Shabala, S. (2014). Polyamines control of cation transport across plant membranes: implications for ion homeostasis and abiotic stress signaling. *Front Plant Sci, 5*, 154. doi: 10.3389/fpls.2014.00154

Reape, T. J., Molony, E. M., & McCabe, P. F. (2008). Programmed cell death in plants: distinguishing between different modes. *Journal of Experimental Botany, 59*(3), 435-444. doi: 10.1093/jxb/erm258

Robinson, K. S., & Aw, R. (2016). The Commonalities in Bacterial Effector Inhibition of Apoptosis. *Trends Microbiol, 24*(8), 665-680. doi: 10.1016/j.tim.2016.04.002

Rodrigo, G., Zwart, M. P., & Elena, S. F. (2014). Onset of virus systemic infection in plants is determined by speed of cell-to-cell movement and number of primary infection foci. *J R Soc Interface, 11*(98), 20140555. doi: 10.1098/rsif.2014.0555

Ruberti, C., Kim, S. J., Stefano, G., & Brandizzi, F. (2015). Unfolded protein response in plants: one master, many questions. *Curr Opin Plant Biol, 27*, 59-66. doi: 10.1016/j.pbi.2015.05.016

Sagor, G. H., Chawla, P., Kim, D. W., Berberich, T., Kojima, S., Niitsu, M., & Kusano, T. (2015). The polyamine spermine induces the unfolded protein response via the MAPK cascade in *Arabidopsis*. *Front Plant Sci, 6*, 687. doi: 10.3389/fpls.2015.00687

Schäfer, P., & Eichmann, R. (2012). The endoplasmic reticulum in plant immunity and cell death. *Frontiers in Plant Science, 3*. doi: 10.3389/fpls.2012.00200

Schneider, C. A., Rasband, W. S., & Eliceiri, K. W. (2012). NIH Image to ImageJ: 25 years of image analysis. *Nat Meth, 9*(7), 671-675.

Schoelz, J. E., Harries, P. A., & Nelson, R. S. (2011). Intracellular transport of plant viruses: finding the door out of the cell. *Mol Plant, 4*(5), 813-831. doi: 10.1093/mp/ssr070

Serrano, C., Gonzalez-Cruz, J., Jauregui, F., Medina, C., Mancilla, P., Matus, J. T., & Arce-Johnson, P. (2008). Genetic and histological studies on the delayed systemic movement of *Tobacco Mosaic Virus* in *Arabidopsis thaliana*. *BMC Genet, 9*, 59. doi: 10.1186/1471-2156-9-59

Silva, M. S., Wellink, J., Goldbach, R. W., & van Lent, J. W. (2002). Phloem loading and unloading of *Cowpea mosaic virus* in *Vigna unguiculata*. *J Gen Virol, 83*(Pt 6), 1493-1504. doi: 10.1099/0022-1317-83-6-1493

Solovyev, A. G., Kalinina, N. O., & Morozov, S. Y. (2012). Recent Advances in Research of Plant Virus Movement Mediated by Triple Gene Block. *Front Plant Sci, 3*, 276. doi: 10.3389/fpls.2012.00276

Sorel, M., Garcia, J. A., & German-Retana, S. (2014a). The Potyviridae Cylindrical Inclusion Helicase: A Key Multipartner and Multifunctional Protein. *Molecular Plant-Microbe Interactions, 27*(3), 215-226. doi: 10.1094/MPMI-11-13-0333-CR

Sorel, M., Svanella-Dumas, L., Candresse, T., Acelin, G., Pitarch, A., Houvenaghel, M. C., & German-Retana, S. (2014b). Key mutations in the cylindrical inclusion involved in *Lettuce mosaic virus* adaptation to eIF4E-mediated resistance in lettuce. *Mol Plant Microbe Interact, 27*(9), 1014-1024. doi: 10.1094/mpmi-04-14-0111-r

Spetz, C., & Valkonen, J. P. (2004). Potyviral 6K2 protein long-distance movement and symptom-induction functions are independent and host-specific. *Mol Plant Microbe Interact, 17*(5), 502-510. doi: 10.1094/mpmi.2004.17.5.502

Srivastava, R., Deng, Y., Shah, S., Rao, A. G., & Howell, S. H. (2013). BINDING PROTEIN is a master regulator of the endoplasmic reticulum stress sensor/transducer bZIP28 in *Arabidopsis*. *Plant Cell, 25*(4), 1416-1429. doi: 10.1105/tpc.113.110684

Tilsner, J., Linnik, O., Louveaux, M., Roberts, I. M., Chapman, S. N., & Oparka, K. J. (2013). Replication and trafficking of a plant virus are coupled at the entrances of plasmodesmata. *J Cell Biol, 201*(7), 981-995. doi: 10.1083/jcb.201304003

Tilsner, J., & Oparka, K. J. (2012). Missing links? - The connection between replication and movement of plant RNA viruses. *Curr Opin Virol, 2*(6), 705-711. doi: 10.1016/j.coviro.2012.09.007

Vassilakos, N., Simon, V., Tzima, A., Johansen, E., & Moury, B. (2016). Genetic Determinism and Evolutionary Reconstruction of a Host Jump in a Plant Virus. *Mol Biol Evol, 33*(2), 541-553. doi: 10.1093/molbev/msv222

Verchot-Lubicz, J., Ye, C. M., & Bamunusinghe, D. (2007). Molecular biology of potexviruses: recent advances. *J Gen Virol, 88*(Pt 6), 1643-1655. doi: 10.1099/vir.0.82667-0

Verchot, J. (2016). How does the stressed out ER find relief during virus infection? *Current Opinion in Virology, 17*, 74-79. doi: http://dx.doi.org/10.1016/j.coviro.2016.01.018

Wan, S., & Jiang, L. (2016). Endoplasmic reticulum (ER) stress and the unfolded protein response (UPR) in plants. *Protoplasma, 253*(3), 753-764. doi: 10.1007/s00709-015-0842-1

Wei, T., Zhang, C., Hong, J., Xiong, R., Kasschau, K. D., Zhou, X., Carrington, J. C., & Wang, A. (2010). Formation of complexes at plasmodesmata for potyvirus intercellular movement is mediated by the viral protein P3N-PIPO. *PLoS Pathog, 6*(6), e1000962. doi: 10.1371/journal.ppat.1000962

Weis, C., Huckelhoven, R., & Eichmann, R. (2013). LIFEGUARD proteins support plant colonization by biotrophic powdery mildew fungi. *J Exp Bot, 64*(12), 3855-3867. doi: 10.1093/jxb/ert217

Williams, B., Verchot, J., & Dickman, M. (2014a). When Supply Does Not Meet Demand-ER Stress and Plant Programmed Cell Death. *Frontiers in Plant Science, 5*. doi: 10.3389/fpls.2014.00211

Williams, B., Verchot, J., & Dickman, M. B. (2014b). When supply does not meet demand-ER stress and plant programmed cell death. *Front Plant Sci, 5*(211). doi: 10.3389/fpls.2014.00211

Williams., Kabbage, M., Britt, R., & Dickman, M. B. (2010). AtBAG7, an *Arabidopsis* Bcl-2-associated athanogene, resides in the endoplasmic reticulum and is involved in the unfolded protein response. *Proc Natl Acad Sci U S A, 107*(13), 6088-6093. doi: 10.1073/pnas.0912670107

Yang, L., Xu, Y., Liu, Y., Meng, D., Jin, T., & Zhou, X. (2016). HC-Pro viral suppressor from tobacco vein banding mosaic virus interferes with DNA methylation and activates the salicylic acid pathway. *Virology, 497*, 244-250. doi: 10.1016/j.virol.2016.07.024

Ye, C., Chen, S., Payton, M., Dickman, M. B., & Verchot, J. (2013). TGBp3 triggers the unfolded protein response and SKP1-dependent programmed cell death. *Mol Plant Pathol, 14*(3), 241-255. doi: 10.1111/mpp.12000

Ye, C., Dickman, M. B., Whitham, S. A., Payton, M., & Verchot, J. (2011). The unfolded protein response is triggered by a plant viral movement protein. *Plant Physiol, 156*(2), 741-755. doi: 10.1104/pp.111.174110

Zhang, L., Chen, H., Brandizzi, F., Verchot, J., & Wang, A. (2015). The UPR branch IRE1-bZIP60 in plants plays an essential role in viral infection and is complementary to the only UPR pathway in yeast. *PLoS Genet, 11*(4), e1005164. doi: 10.1371/journal.pgen.1005164

VITA

OMAR PAUL ARIAS GAGUANCELA

Candidate for the Degree of

Master of Science

Thesis: VIRUS-INDUCED ER STRESS IN PLANTS

Major Field: Entomology and Plant Pathology

Biographical:

   Education:

      Completed the requirements for the Master of Science in Plant
      Pathology at Oklahoma State University, Stillwater, Oklahoma in July,
      2017

      Completed the requirements for the Bachelor of Science in
      Biotechnology at University of the Armed Forces - ESPE, Quito,
      Ecuador in 2014

   Experience:

      Graduate Research Assistant, Department of Entomology and Plant
      Pathology, Oklahoma State University, Stillwater, OK, August 2015 to
      July 2017

      Undergraduate Research Assistant, Department of Entomology and
      Plant Pathology, Oklahoma State University, Stillwater, OK, February
      2014 to June 2014

      Undergraduate Research Assistant, Department of Entomology and
      Plant Pathology, Oklahoma State University, Stillwater, OK, January
      2013 to March 2013